DEVELOPMENT OF SILICON NITRIDE OF IMPROVED TOUGHNESS

by J.J./Brennan

October 2, 1979

UNITED TECHNOLOGIES RESEARCH CENTER

prepared for
NATIONAL AERONAUTICS AND SPACE ADMINISTRATION

FINAL REPORT.

1. Report No. NASA CR-159676	2. Government Accession No.	3. Recipient's Catalog No.
4. Title and Subtitle DEVELOPMENT OF SILICON NITRIDE OF IMPROVED TOUGHNESS		5. Report Date October 2, 1979
		6. Performing Organization Code
7. Author(s) J. J. Brennan		8. Performing Organization Report No. R79-914364-12
		10. Work Unit No.
9. Performing Organization Name and Address United Technologies Research Center East Hartford, CT 06108		
		11. Contract or Grant No. NAS3-21375
		13. Type of Report and Period Covered Contractor Report – Final
12. Sponsoring Agency Name and Address National Aeronautics and Space Administration Washington, DC 20546		
		14. Sponsoring Agency Code

15. Supplementary Notes

Final Report – Project Manager, William A. Sanders, NASA-Lewis Research Center and
Propulsion Laboratory, U.S. Army Research & Technology Laboratories
Cleveland, OH 44135

16. Abstract

The application of reaction sintered Si_3N_4 energy absorbing surface layers to hot-pressed Si_3N_4 was investigated. The surface layer was formed by in-place nitridation of silicon powder. It was found that reaction sintered Si_3N_4 layers of 1 mm thickness, fabricated from either -100, +200, -200, or -325 mesh Si powder and nitrided in 96% N_2/4% H_2 so that ~20-25 vol % unnitrided Si remained in the layer, resulted in a sevenfold increase in ballistic impact resistance of a 0.64 cm thick hot-pressed Si_3N_4 substrate from RT to 1370°C. Both NC-132 Si_3N_4, with MgO additive, and NCX-34 Si_3N_4, with Y_2O_3 additive, were evaluated as substrate material. The finer grain size -200 and -325 mesh nitrided Si layers were found to be preferable for their smoothness and relatively high density. It was found that nitriding in N_2/H_2 mixtures, rather than pure N_2, resulted in a microstructure that did not substantially degrade the strength of the hot-pressed Si_3N_4 substrate.

Thermal cycling tests on the RSSN/HPSN combinations from 200°C to 1370°C for 75 cycles in air did not degrade the impact resistance nor the interfacial bonding, although a large amount of internal silica formation occurred within the RSSN layer. Mach 0.8, 5 hr, hot gas erosion tests showed no surface recession of RSSN layers at 1200°C and slight surface recession at 1370°C.

The formation of an oxidation and erosion protective CVD Si_3N_4 overlayer on the RSSN layers was not successful due to interaction between the residual Si and the deposition process. CVD SiC overlayers were successfully fabricated and, while not optimized, showed excellent thermal cycling and hot gas erosion resistance.

In addition, a brief study was conducted on the severe oxidation problem in the temperature range 700-1000°C of the NCX-34 Si_3N_4 (Y_2O_3) material used in this program.

17. Key Words (Suggested by Author(s)) Ceramics for Gas Turbines Silicon Nitride Impact Resistance Improvement Energy Absorbing Surface Layers Silicon Nitride Ballistic Impact Properties	18. Distribution Statement Unclassified – Unlimited	
19. Security Classif. (of this report) Unclassified	20. Security Classif. (of this page) Unclassified	21. No. of Pages 107	22. Price*

<u>Development of Silicon Nitride of Improved Toughness</u>

TABLE OF CONTENTS

TABLE OF CONTENTS (Cont'd)

I. INTRODUCTION

The application of refractory ceramic materials, in particular Si_3N_4 and SiC, for use in advanced gas turbine engines has recently been an extremely active area of interest. Both Si_3N_4 and SiC have exhibited excellent properties in the areas of strength, thermal shock, creep resistance, and oxidation resistance. However, the use of these materials in certain critical gas turbine applications may be severely limited due to their very low fracture toughness (i.e., resistance to impact damage). Thus, it is imperative to improve the toughness of these materials without sacrificing or compromising their good mechanical and thermal properties.

Various research programs having the objective of improving the impact resistance of Si_3N_4 and SiC have been completed during the last few years. These programs were based on three general approaches:

(1) Improving the impact resistance by fiber reinforcement (Refs. 1-3).

(2) Improving the strength and impact resistance by compressive surface layers (Refs. 4-6,10).

(3) Improving the impact resistance by energy absorbing surface layers (Refs. 1,7-10).

The first of these approaches was previously studied at United Technologies Research Center with excellent results for improving the impact resistance of hot-pressed Si_3N_4 through the use of tantalum wire reinforcement. The second and, in particular, the third of these approaches was studied in a recent NASA contract NAS3-19731 (Ref. 10), the highlights of which are given in the following section of this report. From the results of this previous work, it was decided to concentrate efforts in the current contract on improving the impact resistance of hot-pressed Si_3N_4 through the use of energy absorbing surface layers of porous reaction sintered Si_3N_4.

The objective of this program is to improve the toughness of Si_3N_4 by the development and control of the process of formation of an energy absorbing Si_3N_4 surface layer on a dense Si_3N_4 substrate by in-place nitridation of silicon powder. The program is divided into two tasks:

Task I - Development of Reaction Sintered Si_3N_4 (RSSN) Energy
          Absorbing Surface Layers on Hot-Pressed Si_3N_4

Task II - Effect of Thermal Exposures on R.S. Si_3N_4 - H.P. Si_3N_4
          Combinations With and Without Overlayers of Chemically
          Vapor-Deposited (CVD) Si_3N_4.

II. BACKGROUND

The use of energy absorbing surface layers of porous Si_3N_4 on dense hot-pressed Si_3N_4 in order to improve impact resistance was first studied under the recently completed contract NAS3-19731 (Ref. 10). It was anticipated that surface layers of this type could be expected to absorb energy upon impact due to crushing and crack diversion.

Charpy and ballistic impact specimens of R.S. Si_3N_4 layers on NC-132 Si_3N_4 were fabricated in situ by nitriding a layer of silicon metal powder that had been applied using a water or toluene based slurry. The types of R.S. Si_3N_4 surface layers investigated varied from relatively dense (70%), fine-grained R.S. Si_3N_4 made from -325 mesh Si powder to quite porous (55% dense), large particle-sized layers made from -100, +200 mesh Si powder.

The results of Charpy impact tests at RT and 1370°C showed that the nitrided -200 Si and -325 Si layers on NC-132 Si_3N_4 did not increase the Charpy impact resistance significantly over Si_3N_4 control values. In contrast to the nitrided -325 Si and -200 Si layers, however, the higher porosity large grain size nitrided -100, +200 Si layers on NC-132 Si_3N_4 exhibited Charpy impact energies $2\frac{1}{2}$ times NC-132 Si_3N_4 controls at RT and slightly over twice that recorded for Si_3N_4 controls at 1370°C. From the instrumented Charpy impact load vs time curve it was evident that crushing of the R.S. Si_3N_4 layer occurred during impact.

Ballistic impact tests at RT and 1370°C of R.S. Si_3N_4 layers on NC-132 Si_3N_4 resulted in a fivefold to sixfold improvement in impact energy before substrate failure for nitrided -100, +200 Si and -200 Si layers but only a two to threefold improvement for nitrided -325 Si layers over NC-132 Si_3N_4 control values. To realize optimum energy absorption during a ballistic impact event, it was thought that a combination of porosity and fairly large particle size was necessary to allow crushing of the R.S. Si_3N_4 layer but at the same time, be somewhat resistant to penetration by the projectile.

In order to evaluate the effect of the R.S. Si_3N_4 energy absorbing surface layers on the strength of the NC-132 Si_3N_4 when the interface between the R.S. Si_3N_4 and NC-132 Si_3N_4 is subjected to tensile (bending) stresses, a series of Charpy impact tests were performed with the samples impacted on the side opposite the R.S. Si_3N_4 layer. The results of these tests showed that well bonded R.S. Si_3N_4 layers degraded the Charpy impact strength and bend strength of the NC-132 Si_3N_4 by up to 50%. In general, the large particle and pore size nitrided -100, +200 Si layers degraded the strength more than the smaller particle and pore size nitrided -325 Si layers. The possibility that the degradation is due to the large pores in the R.S. Si_3N_4 layer near the interface acting as stress concentrating flaws suggested that minimizing pore size at the R.S. Si_3N_4/H.P. Si_3N_4 interface by using a graded density R.S. Si_3N_4 layer could possibly help alleviate this problem.

2

Thermal cycling of R.S. Si_3N_4 surface layers on NC-132 Si_3N_4 between 200°C and 1370°C in air for up to 50 cycles resulted in a large amount of silica formation in the high surface area nitrided -325 Si layers that caused debonding at the R.S. Si_3N_4/H.P. Si_3N_4 interface possibly due to thermal expansion mismatch between the silica and the NC-132 Si_3N_4. The larger particle size nitrided -100, +200 Si layers did not form sufficient silica to cause debonding during thermal cycling with the result that the ballistic impact resistance of these cycled layers was the same as noncycled layers at RT and mugh higher at 1370°C. The increase at elevated temperature may be due to plastic deformation of the silica during the high temperature ballistic impact event. For a practical R.S. Si_3N_4 energy absorbing surface layer that must operate in a gas turbine environment, it may be necessary to have an outer layer of dense, impermeable CVD Si_3N_4 covering the R.S. Si_3N_4 surface to add oxidation and possibly erosion resistance.

III. SUMMARY

The development of Si_3N_4 of improved toughness was accomplished by the investigation of reaction sintered Si_3N_4 (RSSN) energy absorbing surface layers on hot-pressed Si_3N_4 (HPSN) by in-place nitridation of silicon powder. Two types of HPSN substrates were used, NC-132 Si_3N_4 with MgO additive and NCX-34 Si_3N_4 with Y_2O_3 additive. Three different particle size Si powders were evaluated: -100, +200 mesh, -200 mesh, and -325 mesh. The toughness increase due to the presence of the 1 mm thick RSSN layers was measured through the use of a ballistic impact test at RT and 1370°C. The effect of the RSSN layer on the strength of the HPSN substrate was measured at RT through the use of a 4-pt bend test with the RSSN layer on the tensile side of the sample.

During characterization of the NCX-34 Si_3N_4 it was found that this particular lot of material undergoes excessive oxidation and resultant loss in strength after 48 hrs at 700-1000°C in air even though NCX-34 material studied previously was very good in low temperature oxidation. It was also found that this lot of material contained 7.15 w/o Y (9.1 w/o Y_2O_3) which is higher than the value of 8.0 w/o Y_2O_3 that according to Norton Co. should be present in NCX-34 Si_3N_4. Furthermore, the Y_2O_3 content varied considerably throughout the billet. It was noted, however, that if this material was subjected to a standard nitriding cycle to 1375°C for 60 hrs in N_2, on subsequent oxidation for 190 hrs at 930°C no weight gain occurred and the strength of the material actually increased. However, at lower temperatures (730°C), disastrous oxidation still occurs but at a much slower rate. Due to the oxidation problems of NCX-34 Si_3N_4 that were encountered during this and other programs, the Norton Co. withdrew this material from the commercial market. The problem of NCX-34 Si_3N_4 further emphasizes the fact that the Si_3N_4-Y_2O_3-SiO_2 system is not fully understood and that continued investigation is necessary to identify the processing parameters and phase relationships in the system that control most of the thermal and mechanical properties.

The RT 4-pt bend strength and the RT and 1370°C ballistic impact strength of NCX-34 and NC-132 Si_3N_4 control samples was determined. The RT 4-pt bend strength of 848 MPa (123 ksi) for the NCX-34 was 25% higher than the NC-132 Si_3N_4. The RT ballistic impact resistance for the NCX-34 of 2.8 joules (2.1 ft-lbs) was almost 50% higher than the NC-132 Si_3N_4, while the 1370°C ballistic impact resistance of both types of Si_3N_4 was approximately the same.

In order to evaluate the effect of energy absorbing surface layers of RSSN on the strength of the hot-pressed Si_3N_4 substrate, a series of nitriding runs in pure N_2 under different nitriding conditions was done, using both -325 mesh and -100, +200 mesh Si powder layers on NC-132 Si_3N_4 substrates. These tests showed that nitriding conditions that resulted in substantial conversion of Si to

Si_3N_4 (1370°C, 24 hrs) resulted in severe strength degradation (~325 MPa) of the NC-132 Si_3N_4 when the layered side was tested in tension, while nitriding conditions of 1250°C, 24 hrs that resulted in only slight conversion of Si to Si_3N_4 (~10%) did not lead to strength degradation of the Si_3N_4 substrate. Examination of fracture surfaces revealed that the fracture origin of degraded samples appeared to be small voids within the RSSN layer lying very close to the RSSN/HPSN interface.

RT 4-pt bend tests of NCX-34 Si_3N_4, nitrided to 1375°C for 60 hrs in N_2, with well bonded RSSN surface layers indicated that, as previously found for NC-132 Si_3N_4, the nitriding of the Si powder layers introduces strength limiting flaws at the HPSN/RSSN interface that result in a 40-50% drop in bend strength when the nitrided layer is tested in tension. Nitriding tests with Si powder lightly sprinkled on the NCX-34 tensile surfaces showed that the fracture origin of degraded samples was always associated with a nitrided particle of Si or a depression that appeared to be at one time associated with a nitrided Si particle.

However, results of 4-pt bend tests on NC-132 and NCX-34 Si_3N_4 with RSSN layers of various purity nitrided in a N_2/H_2 mixture indicate that a minimal amount of substrate degradation occurs for well bonded layers of 98% purity -325 Si and -200 Si on both NCX-34 and NC-132 Si_3N_4. Nitriding in N_2/H_2 mixtures (96% N_2/4% H_2) also led to a much faster rate of conversion of the Si to Si_3N_4 and an α to β-Si_3N_4 ratio of ~2:1, whereas nitriding in 100% N_2 gave an RSSN product of ~70% β, 30% α. The much greater amount of α-Si_3N_4, which forms primarily as fine whisker-like crystals interconnecting the β-Si_3N_4 grains, may be responsible for the lesser amount of substrate degradation observed for the samples nitrided in N_2/H_2 mixtures, due to the α-Si_3N_4 whisker mat not allowing the β-Si_3N_4 grains to bond directly to each other or to the HPSN substrate. Thus, no large stress-concentrating flaws are bonded directly to the HPSN surface and cracks initiating in the RSSN layer cannot propagate directly through β-Si_3N_4 grains and into the HPSN substrate.

Ballistic impact tests at RT and 1370°C on NCX-34 Si_3N_4 substrates with RSSN layers fabricated from both -325 and -100, +200 Si powder indicated that fully nitrided RSSN layers (i.e., no residual Si) result in only modest (50-100%) improvement in impact resistance. To obtain optimum impact resistance of over 11 joules (8 ft-lbs), as previously found for -100, +200 Si RSSN layers on NC-132 Si_3N_4, a certain amount of residual silicon within the RSSN particles appears to be necessary. However, enough Si_3N_4 must be formed to strongly bond the particles to one another. For -100, +200 Si RSSN layers the optimum amount of residual Si for excellent ballistic impact resistance was found to be in the range of 15-25 vol %.

5

In order to obtain an RSSN energy absorbing layer with a smoother surface finish, -325 and -200 mesh Si powder was used to form RSSN layers containing residual Si. From nitriding experiments conducted first in 100% N_2 and later in 96% N_2/4% H_2 on both NC-132 and NCX-34 Si_3N_4 substrates, it was found that a residual Si content of >20 vol % was necessary for optimum ballistic impact resistance. The highest RT ballistic impact resistance ever recorded during the course of this program of 14.5 ft-lbs (19.7 joules) was obtained for -325 Si RSSN layers on NCX-34 Si_3N_4 substrates that were nitrided in a 96% N_2/4% H_2 mixture according to a schedule that resulted in ~20 vol % residual Si in the RSSN layer. The program goal of 7 ft-lbs (9.5 joules) at RT and 1370°C was met and exceeded for ballistic impact samples of -325 and -200 Si layers, nitrided in N_2/H_2 to yield 20 vol % residual Si, on either NC-132 or NCX-34 Si_3N_4 substrates. The residual Si is apparently absorbing a great deal of energy as it is crushed and fractured by the ballistic projectile.

Task II of this program consisted of evaluating the effect of thermal cycling on the integrity of the RSSN/HPSN combinations, in particular the effect of silica formation within the RSSN layer on its ability to absorb energy during ballistic impact. To minimize silica formation, an oxidation barrier of CVD Si_3N_4 on top of the RSSN layer was also to be evaluated. In addition, the hot gas erosion characteristics of the RSSN layers at 1200 and 1370°C in a Mach 0.8 gas stream were evaluated, both with and without a thin CVD Si_3N_4 overlayer.

It was found that thermal cycling 75 times between 150-200°C to either 1200 or 1370°C does not adversely affect the ballistic impact resistance of NC-132 or NCX-34 Si_3N_4 control samples, tested at RT and 1370°C. Ballistic samples of NC-132 or NCX-34 Si_3N_4 with -325 or -200 RSSN layers containing ~25 vol % residual Si, when cycled 75 times between 150 and 1200°C or 200 and 1370°C, actually register an increase in ballistic impact resistance when tested, especially at 1370°C. The increase at 1370°C is undoubtedly due to the large amount of SiO_2 formed within the RSSN layers during cycling that is deforming plastically during impact. Even though large amounts of cristobalite (SiO_2) were formed within the RSSN layer during thermal cycling, it did not affect the bonding between the RSSN layer and the HPSN substrate. Also, the cristobalite formed mainly at the expense of the α-Si_3N_4 within the RSSN layer and thus did not reduce the residual Si content below the critical 20 vol % level.

Attempts to form a protective CVD Si_3N_4 overlayer on RSSN layers containing ~25 vol % Si were unsuccessful due to the interference of the Si with the deposition process. CVD Si_3N_4 could only be deposited at temperatures of 1400°C or greater and at these temperatures pinholes were formed in the layer over residual Si particles. Attempts to deposit CVD Si_3N_4 at lower temperatures, where the Si vapor pressure would not be as high, were unsuccessful.

6

However, CVD SiC, which can be deposited at temperatures of 1100-1150°C, was successfully deposited on -200 RSSN layers. CVD SiC overlayers thicker than ~50μ (2 mils) tended to crack severely on cooling from deposition due to thermal expansion mismatch, and on subsequent thermal cycling tended to spall, offering no protection from oxidation. CVD SiC overlayers of 12-25μ (0.5-1.0 mils) in thickness were deposited crack-free and, on thermal cycling, did offer substantial oxidation protection and no decrease in ballistic impact properties. While some internal oxidation of the RSSN layer still occurred, it is felt that an optimized CVD SiC overlayer could be extremely oxidation resistant.

Mach 0.8, 5 hr, hot gas erosion testing at sample temperatures of 1200°C and 1370°C were run on NC-132 and NCX-34 Si_3N_4 controls and on samples with -200 and -325 RSSN layers (25 vol % Si), both with and without CVD Si_3N_4 overlayers. For the Si_3N_4 controls, no surface recession or weight change was observed at 1200°C, while at 1370°C a very slight surface recession (2.5μ) and weight gain (+0.1 mg) was observed for NC-132 Si_3N_4 and a rather large surface recession (25μ) and weight loss (-3.5 mg) for NCX-34 Si_3N_4. For the -325 and -200 RSSN layers, no surface recession was detected at 1200°C but there was a substantial weight gain (~20 mg) due to the formation of silica on and within the RSSN layers. Samples with CVD Si_3N_4 overlayers also exhibited ~20 mg weight gains, indicating that the CVD layer was not protecting the RSSN from oxidation, although no oxidation product was detected on the CVD Si_3N_4 surface. At 1370°C, the -325 and -200 RSSN layers did exhibit a small surface recession (~8μ) and a substantial weight gain (~12 mg). The samples with CVD Si_3N_4 overlayers again gained substantial weight but did not exhibit any measurable surface recession, indicating that the CVD Si_3N_4 layer is very erosion resistant even though it is not completely continuous over the RSSN surface.

Hot gas erosion tests of samples of NCX-34 and NC-132 Si_3N_4 with -200 RSSN layers (25 vol % Si) and overlayers of CVD SiC of 36μ (1.5 mil) thickness showed that these overlayers were very resistant to surface recession and relatively good in oxidation protection. Compared to the CVD Si_3N_4, samples with CVD SiC overlayers gained less than 25% of the weight. Again, it is felt that an optimized CVD SiC overlayer could offer excellent oxidation and erosion protection for RSSN energy absorbing surface layers on hot-pressed Si_3N_4 substrates.

7

IV. TECHNICAL PROGRESS SUMMARY

4.1 Fabrication and Characterization of Specimens

4.1.1 Fabrication and Characterization of Hot-Pressed Si_3N_4 Substrate Material

The silicon nitride samples used in this investigation consist of Norton Co. hot-pressed Si_3N_4, both NC-132 with MgO additive and NCX-34 with Y_2O_3 additive. Bend specimens of dimensions 4.44 x 0.508 x 0.254 cm (1.75 x 0.200 x 0.100 in.) and ballistic impact specimens of dimensions 3.81 x 2.54 x 0.64 cm (1.50 x 1.00 x 0.25 in.) of both types were machined from 15.3 x 15.3 x 2.54 cm (6 x 6 x 1 in.) billets. The wide (0.508 x 4.44 cm) face of the bend specimen and the narrow (0.64 x 3.81 cm) face of the ballistic impact specimen were perpendicular to the billet hot press direction.

Randomly selected specimens from each billet were characterized as to density, grain size, impurity content, and surface defects. The grain size and morphology was determined by replication techniques using the electron microscope. Impurity content was determined by spectrochemical analysis. Zyglo dye penetrant inspection was used to detect surface cracks or pits.

The impurity content of the NC-132 and NCX-34 Si_3N_4 materials, along with their densities, is given in Table I. The major impurities in NC-132 Si_3N_4 are Al, Fe, Mg, and W. The Mg is added deliberately as MgO for densification purposes while the W is present as WSi_2, resulting from WC pickup during milling of the powder prior to hot pressing. The major impurities in NCX-34 Si_3N_4 are Fe, W, and Y. In this material, the Y is added deliberately as Y_2O_3 for densification purposes. It is interesting to note that 7.15 w/o Y corresponds to 9.1% Y_2O_3, more than the 8.0 w/o Y_2O_3 that, according to Norton Co., is supposed to be present in the NCX-34 material. Subsequent chemical analysis of billet #F338355, which was machined into 4-pt bend samples, indicated that the yttrium content varied throughout the billet with the Y_2O_3 content ranging from 7.6 to 9.4%. The grain size and morphology of the NCX-34 and NC-132 Si_3N_4 can be seen from Fig. 1 and Table II. While the Si_3N_4 grain size and morphology is similar for the two materials, their etching characteristics (hot HF) are quite different, which is indicative of different grain boundary phases. The NC-132 Si_3N_4 etched very readily due to the magnesium silicate glassy phase that is present at grain boundaries and triple points. The NCX-34 material was very difficult to etch with very little etching occurring except for rather large areas of what appears to be a second crystalline phase, probably "H" phase ($Y_{10}Si_6O_{24}N_2$). "H" phase was detected by X-ray analysis as well, and appears to be present in the amount of approximately 9 vol %.

8

All of the NCX-34 Si_3N_4 samples cut from the three billets ordered from the Norton Co. exhibited a macrostructure that was visible to the naked eye. This macrostructure consisted of a lighter colored skeletal structure interspersed with dark regions. On immersion in Zyglo dye penetrant with subsequent examination under U.V. light, the light areas pick up the penetrant while the dark areas do not (Fig. 2). Although the NCX-34 Si_3N_4 samples appear to contain either porosity or very small cracks, 4-pt bend tests conducted at RT gave a strength of 848 MPa (123 ksi), which is 25% higher than that recorded for NC-132 Si_3N_4. Thus, the defects in NCX-34 Si_3N_4 that are visible from Zyglo dye penetrant inspection, do not appear to compromise the strength properties of the material, at least at RT.

Included in the characterization study of NCX-34 Si_3N_4 were oxidation studies in the 700-1000°C range, since some Si_3N_4-Y_2O_3 materials have been known to exhibit poor oxidation properties in this temperature range. Previous studies at UTRC and Norton Co. indicated that the NCX-34 Si_3N_4 material did not exhibit oxidation problems in this temperature range. However, tests on the recently delivered material, in particular the bend specimens cut from billet #F338355 which contained 7.15 w/o Y, showed that after oxidation at 930°C for 100 hrs in air, the samples gained over 1 mg/cm^2 and suffered a reduction in strength from 848 MPa (123 ksi) to 675 MPa (98 ksi). The lighter colored areas started to turn very white after a few hours while some, but not all, of the darker areas remained quite dark, as shown in Fig. 3. After 150 hrs at 930°C a few samples became degraded to the point of exhibiting essentially no strength. Aging the NCX-34 Si_3N_4 material at 730°C in air produced even more pronounced degradation, with samples literally falling apart after only 48 hrs, as shown in Fig. 4.

An interesting sidelight to the oxidation characteristics of the NCX-34 Si_3N_4 is that samples that had been put through a nitriding cycle to 1375°C in N_2 for 60 hrs, while exhibiting a loss in strength due to this cycle from 848 MPa (123 ksi) to 725 MPa (105 ksi), did not gain any measurable weight when subsequently oxidized for 190 hrs at 930°C and actually exhibited an increase in strength to 930 MPa (135 ksi). Gazza, et al (Ref. 11) noted similar behavior for Si_3N_4 + 13 w/o Y_2O_3 samples nitrided in N_2/H_2 mixtures and subsequently oxidized at 1000°C. The mechanism responsible for this "healing" effect for oxidation prone Si_3N_4-Y_2O_3 materials is unknown at this time; however, it does not prevent disastrous oxidation from occurring at lower temperatures. A series of nitriding runs were conducted using both pure N_2 and 96% N_2/4% H_2 mixtures for periods up to 65 hrs at 1375°C with subsequent oxidation at 730°C. While the NCX-34 Si_3N_4 samples put through the nitriding cycles did not degrade as rapidly as "as-received" samples during the subsequent 730°C oxidation treatment, they eventually did degrade. It took approximately 48 hrs at 730°C for visual cracks to form in the nitrided samples compared to less than 10 hrs in the as-received NCX-34 Si_3N_4.

Although the low temperature oxidation problems of the NCX-34 Si_3N_4 procured for this program were extremely serious, and led the Norton Co. to remove the material from the commercial market, this phenomonon could not be studied further under the scope of the present contract. However, it was decided to use the material along with NC-132 Si_3N_4 as a substrate for the evaluation of energy absorbing surface layers of reaction sintered Si_3N_4 (RSSN). The reason for this decision was that all testing under the program was to be done either at RT or $1370^{\circ}C$, and the material was found to exhibit excellent strength properties at these temperatures. However, the problem of NCX-34 Si_3N_4 further emphasizes the fact that the Si_3N_4-Y_2O_3-SiO_2 system is not fully understood and that continued investigation is necessary to identify the processing parameters and phase relationships in the system that control most of the thermal and mechanical properties.

4.1.2 Fabrication and Characterization of RSSN/HPSN Combinations

The RSSN energy absorbing surface layers were fabricated in situ on ballistic impact and 4-pt bend samples of hot-pressed Si_3N_4 by nitriding a layer of Si powder applied to the sample from a liquid slurry. The Si powders used were purchased from Cerac, Inc. and consisted of two -325 mesh powders of 98% and 99.6% purities, a -200 mesh powder of 98.5% purity, and a -100, +200 mesh powder of 98.5% purity. The chemical analysis of the four powders used is given in Table III. The major impurities in the 98% and 98.5% pure powders consist of Fe, Al, Mn, and Ca. The major impurities in the -325 (99.6%) powder are Al and Pb. The surface area of the finer powders was also determined by the BET method. The results of this analysis are given in Table IV and show that the surface area of the -325 (98%) powder is greater than the -200 (98.5%) as would be expected, and that the -325 (99.6%) is substantially greater than the lesser purity -325 mesh powder, which was not expected.

The procedure for fabricating the RSSN layers on the HPSN ballistic and 4-pt bend samples was as follows. The -325 or -200 Si powder was mixed with enough distilled water to form a thick slurry. The -100, +200 mesh powder would not form a slurry with water that, when dried, could be handled without damaging the Si layer, so it was mixed with toluene + 5 wt % polystyrene to form a slurry that had good green strength when dried. The Si powder slurries were then applied to the HPSN samples to form a layer ~1.5 mm thick when dry. The samples were then loaded into Mo boats with loose fitting covers, which were then put into a mullite tube furnace with controlled atmosphere for nitriding. After nitriding, the RSSN layers were surface ground to a uniform thickness of 1 mm. Figure 5 shows three steps in forming an RSSN layer of -200 mesh Si powder on an NC-132 Si_3N_4 ballistic impact sample, starting from the dried Si powder slurry, through the nitriding step, and then the surface grinding. With a more precise method of applying the powder slurry, such as injection molding, the final grinding step would not be necessary.

Density measurements taken on RSSN surface layers have shown that, using the slurry method of fabrication, a fully nitrided −100, +200 Si layer would contain approximately 45% porosity, a −200 Si layer would contain ~30-35% porosity, while the −325 Si layers would contain ~25-30% porosity. Occasionally, large bubbles in the Si slurry would persist in the RSSN layer, creating very large pores. Samples with this type of porosity near the impact point would be rejected from the testing program. Any samples that exhibited poor bonding or cracking between the RSSN layer and the HPSN substrate would also be rejected from further testing. This problem was only encountered with the −325 Si (99.6%) RSSN layers, and even then only infrequently. Representative samples from each nitriding run were subjected to X-ray diffraction analysis in order to determine the relative amounts of α-Si$_3$N$_4$, β-Si$_3$N$_4$, and free Si in the RSSN layer.

4.2 Ballistic Impact Testing

The ballistic impact testing procedure consisted of firing 4.4 mm diameter hardened chrome-steel pellets, weighing 0.34 gms, from a modified Crossman air pistol or rifle (for higher velocities) at the center of the ballistic impact sample protruding from the holding arrangement. The plates of Si$_3$N$_4$ were held at one end in a vise arrangement so that a 2.54 x 2.54 cm (1.0 x 1.0 in.) square 0.64 cm (0.25 in.) thick was available for impact. The pistol and rifle were pressurized by helium, which could be adjusted so that velocities of 99 to 230 m/sec (325 to 755 ft/sec) could be obtained for the pistol and 152 to 343 m/sec (500 to 1125 ft/sec) could be obtained for the rifle. These velocities were measured at a distance of 30 cm (12 in.) from the end of the gun barrel and it was at this distance that the samples were always positioned. The kinetic energy of the steel pellets available for impact could thus be varied from a low of 1.6 joules (1.2 ft-lbs) to a high of 19.7 joules (14.5 ft-lbs).

Ballistic impact tests were performed at RT and 1370°C. The 1370°C tests were done by heating the reverse side of the ballistic impact sample with an oxyacetelene torch until the front side registered a temperature of ~1370°C as read by an optical pyrometer. Control samples of hot-pressed Si$_3$N$_4$ (i.e., those without a RSSN layer) were tested by setting the helium pressure at a value that corresponded to 145 m/sec pellet velocity and then impacting the sample. If the sample did not fracture, the helium pressure was raised in 50 psi increments until failure occurred. Often, five or more impacts would be necessary to fail the sample. Samples with RSSN layers could be impacted only once, since the RSSN layer was usually damaged or destroyed after impact, so that a number of samples were required to establish the velocity necessary to fracture the Si$_3$N$_4$ substrate.

11

4.2.1 Ballistic Impact Testing of Si_3N_4 Controls

Ballistic impact tests were performed on NCX-34 Si_3N_4 controls at RT and 1370°C. NC-132 Si_3N_4 ballistic tests had been done under the previous contract (Ref. 10) and were not repeated, except for a few to verify the previous results. The results of these tests are given in Table V. The average RT impact energy necessary to fail the 25.4 x 38.2 x 6.35 mm (1 x 1½ x 0.25 in.) sample of NCX-34 Si_3N_4 was 2.8 joules (2.1 ft-lbs), compared to NC-132 Si_3N_4 that failed at 1.9 joules (1.4 ft-lbs). The increase in RT ballistic impact resistance of the NCX-34 Si_3N_4 over the NC-132 Si_3N_4 is consistent with the observation that Si_3N_4 densified with Y_2O_3 additive exhibits a significantly higher RT fracture toughness ($K_{IC} \approx 7$ MN/m$^{3/2}$) than Si_3N_4 densified with MgO ($K_{IC} \approx 4.5$ MN/m$^{3/2}$) (Ref. 12).

At 1370°C, the ballistic impact resistance of the NCX-34 Si_3N_4 is approximately the same as at RT, being 2.6 joules (1.9 ft-lbs). This compares favorably to the value of 2.8 joules for NC-132 Si_3N_4 at 1370°C, which for this material is due to energy absorption through plastic deformation of the magnesium silicate grain boundary phase.

The fracture mode for NCX-34 Si_3N_4 is predominantly tensile failure on the reverse side of the sample at RT and indeterminate at 1370°C. At 1370°C, the samples tend to split longitudinally into two pieces with a very smooth fracture surface, whereas at RT they normally shatter into 4 or more pieces with very rough fracture surfaces and very definite fracture origins. In contrast, the NC-132 Si_3N_4 samples fail in a predominantly Hertzian mode at RT and a mixed Hertzian/tensile mode at 1370°C.

4.3 4-Pt Bend Testing of NCX-34 and NC-132 Si_3N_4 Controls

NCX-34 and NC-132 Si_3N_4 bend specimens of dimensions 4.44 x 0.508 x 0.254 cm (1.75 x 0.200 x 0.100 in.) were tested in 4-pt bending at RT. All 4-pt bend testing was done using an inner span of 1.9 cm (0.75 in.) and an outer span of 3.81 cm (1.5 in.) at a crosshead speed of 0.25 cm/min (0.1 in/min). The average bend strength of NCX-34 Si_3N_4 controls was 848 MPa (123 ksi), which was substantially higher than that found for NC-132 Si_3N_4 of 662 MPa (96 ksi). The fracture origin invariably was located at a surface flaw (mostly at corners) introduced by the machining process. All samples had been longitudinally ground with a 400 grit diamond grinding wheel.

4.4 Task I - Development of RSSN Energy Absorbing Surface Layers on
     Hot-Pressed Si_3N_4

Previous work (Ref. 10) had indicated that relatively thin layers (~1 mm)
of reaction sintered Si_3N_4 (RSSN), formed in situ on hot-pressed Si_3N_4 sub-
strates by nitriding a layer of Si powder, increased the ballistic impact resis-
tance of the substrate by up to a factor of seven. The most successful RSSN
layer was fabricated from -100, +200 mesh Si powder. RSSN layers fabricated
from -200 and -325 mesh powder were less successful in increasing impact resis-
tance. It was surmised from this that for maximum impact resistance, a large
grain size, large pore size RSSN layer was necessary.

    4.4.1 Ballistic Impact Testing of RSSN/HPSN Combinations

In order to verify the previous results, which had been obtained using NC-132
Si_3N_4 substrates, a nitriding run was done using NCX-34 ballistic impact samples
with both -325 Si and -100, +200 Si layers. All samples were nitrided in one
run using the standard schedule of 20 hrs at 1150^oC in Ar, 24 hrs at 1250^oC in
N_2, followed by 60 hrs at 1375^oC in N_2. Ballistic impact tests were performed
on these samples at RT and 1370^oC, the results of which are given in Table VI.

From these tests, it was found that the NCX-34 Si_3N_4 with -325 Si nitrided
surface layers could withstand only 6.2 joules at RT and 4.9 joules at 1370^oC
before fracturing. The samples with -100,+200 Si nitrided surface layers with-
stood even less; 4.9 joules at RT and 3.7 joules at 1370^oC. While these values
represent an improvement of 50-125% in ballistic impact resistance over samples
without RSSN layers, they were still much less than found previously for RSSN
layers on NC-132 Si_3N_4. The reason for this appears to be due to the fact that
the RSSN layers in these tests were essentially completely nitrided, even the
-100, +200 Si layers. From X-ray results on the nitrided -100, +200 Si layers,
less than 5 vol % unreacted Si was detected. Photomicrographs of these layers
confirm this finding, as shown in Fig. 6. This figure shows the interface be-
tween the nitrided -100, +200 Si layer (top) and the NCX-34 Si_3N_4 substrate
(bottom). Only the large $\beta-Si_3N_4$ particles with very small amounts of unreacted
Si are evident in the RSSN layer, due to the fact that the resin used to infil-
trate the sample for polishing purposes (dark grey phase) has destroyed most of
the fine $\alpha-Si_3N_4$ needles that exist between the large $\beta-Si_3N_4$ particles. X-ray
analysis indicates that this RSSN layer consists of ~70% β, 30% $\alpha-Si_3N_4$.

Previously tested -100, +200 Si layers on NC-132 Si_3N_4 contained a substan-
tial amount (~15-20 vol %) of unreacted silicon in the interior of the nitrided
particles. The reason for the complete nitridation of the -100, +200 Si powder
particles on NCX-34 Si_3N_4 is not clear, since the standard nitriding schedule
of 20 hrs in Ar at 1150^oC, 24 hrs in N_2 at 1250^oC, and 60 hrs in N_2 at 1375^oC,
has been used almost exclusively throughout the program.

13

In order to evaluate the effect of unreacted Si on the ballistic impact resistance, both NC-132 and NCX-34 Si_3N_4 substrates with layers of -100,+200 Si were nitrided according to the above schedule except that the $1375^{\circ}C$ nitridation step was reduced to 24 hrs. From X-ray analysis and optical microscopy of the nitrided layers, it was found that this nitriding schedule resulted in approximately 25-30 vol % unreacted Si in the interior of the -100, +200 nitrided Si particles, as shown in Fig. 7. The results of RT ballistic impact tests on these samples are given in Table VII.

From Table VII, it can be seen that an impact energy in excess of 9.1 joules is necessary to fracture the NC-132 substrates with over 11.4 joules being necessary to fracture the NCX-34 Si_3N_4 substrates. These results are more in line with previous results for NC-132 Si_3N_4 and are what was anticipated for NCX-34 Si_3N_4, based on its higher ballistic impact resistance at RT over NC-132 Si_3N_4. It thus appears that to obtain maximum ballistic impact resistance from a RSSN layer on dense Si_3N_4, a certain amount of unreacted Si is necessary.

Further nitriding tests were done on ballistic samples of NCX-34 Si_3N_4 with both -325 Si and -100,+200 Si layers using the normal schedule except with only an 8 hr hold at the maximum temperature of $1375^{\circ}C$. A few of the -100,+200 Si samples were placed in the nitriding furnace in such a position that the maximum temperature was only ~$1300^{\circ}C$.

The results of RT ballistic impact rests on the samples nitrided to $1375^{\circ}C$ for 8 hrs are given in Table VIII. As in the case of -100, +200 Si layers nitrided for 24 hrs at $1375^{\circ}C$, an impact energy in excess of 11.4 joules was necessary to fracture the NCX-34 Si_3N_4 substrates. However, the nitrided -325 Si layers could only withstand up to 6.2 joules before the substrate fractured. From X-ray analysis and optical microscopy of the nitrided layers, it was found that the 8 hr, $1375^{\circ}C$ nitriding schedule resulted in approximately 60% unreacted silicon within the large β-Si_3N_4 grains of the -100,+200 Si nitrided layer (Fig. 8), while the -325 Si nitrided layers were essentially completely nitrided (Fig. 9) to a mixture of ~65% β, 35% α-Si_3N_4.

The -100,+200 Si samples that were deliberately nitrided to only $1300^{\circ}C$, 8 hrs, exhibited RT ballistic impact resistance less than the -100,+200 Si samples nitrided to $1375^{\circ}C$, 8 hrs. They were also somewhat friable, indicative of poor particle-to-particle bonding. From X-ray analysis and optical microscopy it was evident that very little of the Si had been converted to Si_3N_4 (~10 vol %), as shown in Fig. 10. Not enough Si_3N_4 had been formed to bond the particles together, thus resulting in the observed friable layer.

It thus appears obvious that some residual silicon must be present in the RSSN layer in order to achieve maximum ballistic impact resistance. However, enough Si_3N_4 must be formed to strongly bond the particles to one another. Since the samples with -100,+200 Si layers containing ~60 vol % residual silicon did not exhibit any greater impact resistance than those with ~25 vol % residual silicon, it would appear that to avoid any possible thermal expansion mismatch problems, only the minimum amount of residual silicon necessary to achieve maximum impact resistance should remain in the RSSN layer. For -100,+200 Si layers this optimum amount of residual silicon appears to be in the range of 15-25 vol %.

4.4.1.1 RT Ballistic Impact Testing of Fine Grained RSSN Layers

Since it appeared that the excellent impact properties of -100, +200 RSSN layers were related to the amount of residual Si present, it was decided to determine if finer grained RSSN layers fabricated from -325 or -200 Si and containing residual Si after nitriding could achieve the same results. To date, almost all of the -325 or -200 Si layers studied have been fully nitrided. The finer grained RSSN layers could offer certain advantages over the -100, +200 Si RSSN layers due to their smoother surfaces and ease of fabrication. Accordingly, nitriding experiments with -325 Si and -200 Si layers on ballistic samples of both NC-132 and NCX-34 Si_3N_4 in N_2 and N_2/H_2 mixtures for varying lengths of time at the maximum nitriding temperature of $1375^{\circ}C$ were run.

The first nitriding experiments were run in pure N_2 for a period of 1 hr at the maximum nitriding temperature of $1375^{\circ}C$. The -200 Si layers nitrided under these conditions appeared to contain approximately 30 vol % unreacted Si, as determined from X-ray analysis and optical microscopy. The determination of the relative amounts of $\alpha-Si_3N_4$, $\beta-Si_3N_4$, and free Si was done using the method of Gazzara, et al (Ref. 13). The -325 layers nitrided under the same conditions contained approximately 20 vol % unreacted Si. The Si_3N_4 in both samples was a mixture of ~55% β, 45% α.

The results of RT ballistic impact tests of NC-132 and NCX-34 Si_3N_4 with the above layers are presented in Table IX. Most of the samples in this nitriding run were NC-132 Si_3N_4 and, from Table IX, it can be seen that both -325 Si and -200 Si RSSN layers on NC-132 Si_3N_4 required an impacting energy of 15.4 joules in order to fracture the substrate. Figure 11 shows the NC-132 Si_3N_4 sample with a -200 Si RSSN layer that was impacted at 230 mps (9.1 joules). Note that the RSSN layer was destroyed only at the point of impact. This value is higher by almost 2 joules than the previously obtained value of 13.6 joules for -100, +200 Si RSSN layers on NC-132 Si_3N_4 that contained ~20 vol % unreacted Si.

15

Only two samples of NCX-34 Si_3N_4 were included in the 1 hr, $1375^{\circ}C$, N_2 nitriding run; one with a -325 Si layer and one with a -200 Si layer. Both of these samples withstood an impacting energy of 15.4 joules without failure of the substrate. This demonstrates once again that, at least at RT, NCX-34 Si_3N_4 has greater ballistic impact tolerance than NC-132 Si_3N_4, both with and without RSSN energy absorbing surface layers.

Since it was found on this program that nitriding in a 96% N_2/4% H_2 atmosphere instead of pure N_2 resulted in minimal strength degradation of both NC-132 and NCX-34 Si_3N_4 when RSSN layers of -325 Si (98%) were tested in 4-pt bending with the layered side in tension, as discussed in a following section, it was decided to continue further short time nitriding tests using the N_2/H_2 mixture as the nitriding media. Accordingly, a repeat of the previous nitriding run of Ar, $1150^{\circ}C$, 20 hrs followed by $1250^{\circ}C$, 24 hrs, in N_2, and then 1 hr at $1375^{\circ}C$ in N_2, was done using 96% N_2/4% H_2 in place of the 100% N_2. Both NC-132 and NCX-34 Si_3N_4 substrates were used with -200 Si layers but only NCX-34 Si_3N_4 was used with -325 Si layers.

From X-ray analysis and optical microscopy it was found that the -200 Si layers contained ~21 vol % residual Si (Fig. 12) down from ~30 vol % for -200 Si layers nitrided in N_2 for 1 hr at $1375^{\circ}C$, while the -325 Si layers contained only ~5 vol % residual Si (Fig. 13) down from ~20 vol % for -325 Si layers nitrided in N_2. It was also found that the microstructure of the layers nitrided in N_2/H_2 mixtures was quite different than the same layers nitrided in 100% N_2. There was much more evidence of fine grained α-Si_3N_4 around the larger β-Si_3N_4 grains. This has also been observed recently by Lindley, et al (Ref. 14). This was substantiated by the X-ray analysis of both the -325 Si and -200 Si layers indicating that the Si_3N_4 present consisted of more α than β; 73% α, 27% β for the -200 Si layers and ~58% α, 42% β for the -325 Si layers. This is in contrast to the same layers nitrided under identical conditions except using 100% N_2, where the β-Si_3N_4 content was always greater than the α-Si_3N_4.

The results of RT ballistic impact tests on these samples are given in Table X. As in the case of -200 Si layers nitrided for 1 hr at $1375^{\circ}C$ in N_2, these layers nitrided in N_2/H_2 under the same conditions resulted in impact energies of 15.4 joules being necessary to fracture the NC-132 Si_3N_4 substrates while 17.2 joules was necessary to fracture the NCX-34 substrates. Figures 14 and 15 show the NCX-34 Si_3N_4/-200 RSSN ballistic samples after 15.4 and 17.2 joule impacts, respectively. However, the -325 Si layers on NCX-34 Si_3N_4, nitrided in N_2/H_2 for 1 hr at $1375^{\circ}C$, and containing only 5 vol % unreacted Si, required a rather low impact energy of 9.1 joules to fracture the substrate. It is thus obvious that more than 5 vol % is necessary in the RSSN layers for maximum impact resistance.

In order to determine the minimum amount of residual Si necessary in RSSN layers on dense Si_3N_4 for maximum impact resistance, further nitriding tests were carried out using –325 and –200 Si powder layers on NCX–34 Si_3N_4 substrates. Samples were nitrided in N_2/H_2 at a maximum temperature of $1375^\circ C$ for periods of 30 min, 1½ hrs, and 2 hrs for the –200 Si layers and for 30 min for the –325 Si layers. Quantitative X-ray analysis showed that for samples nitrided for 30 min at $1375^\circ C$, the –325 Si layers consisted of 20 vol % Si, 55 vol % $\alpha-Si_3N_4$, and 25 vol % $\beta-Si_3N_4$, while the –200 Si layers contained 25 vol % Si, 50 vol % $\alpha-Si_3N_4$, and 25 vol % $\beta-Si_3N_4$. The amount of residual Si in –200 layers nitrided for 1½ hrs was ~14% while those nitrided for 2 hrs was ~6%.

The RT ballistic impact results for these and the previously tested samples nitrided for 1 hr at $1375^\circ C$ are given in a shortened form in Table XI. Only the test results for samples that fall on either side of the energy required to fracture the Si_3N_4 substrate are shown. From Table XI, it is evident that nitriding –200 Si layers in N_2/H_2 for much more than 1 hr at $1375^\circ C$ results in too much conversion of Si to Si_3N_4 with accompanying reduction in ballistic impact resistance. Residual Si content of greater than ~20 vol % does not lead to increases in ballistic impact resistance at RT. For maximum impact resistance with minimum residual Si content for –200 Si RSSN layers, a nitriding schedule of ~1 hr at a maximum temperature of $1375^\circ C$ in a 96% N_2/4% H_2 mixture appears to be optimal.

For the finer grain size –325 Si RSSN layers, a shorter nitriding time at $1375^\circ C$ is necessary for optimum ballistic impact resistance, compared to the –200 Si layers. In fact, –325 Si layers on NCX–34 Si_3N_4 substrates nitrided for 30 min at $1375^\circ C$ in N_2/H_2, when tested at RT in ballistic impact, could not be fractured within the limits of the ballistic impact equipment. The maximum velocity obtainable is 343 m/sec (1125 ft/sec) which is equivalent to an impacting energy of 19.7 joules (14.5 ft-lbs). This energy was insufficient to fracture the above mentioned samples, which represents the highest as-nitrided RT ballistic impact resistance ever recorded under this program.

One additional type of RSSN layer containing ~20 vol % Si was tested in ballistic impact at RT. These layers consist of 75 vol % –325 Si and 25 vol % –100, +200 Si. The nitriding schedule was such that essentially all of the –325 Si was converted to Si_3N_4 while only a small amount of –100, +200 Si particles were reacted. Thus, the layer consisted of a fine grained fully nitrided matrix with large Si particles interspersed throughout. Ballistic impact testing of this type of RSSN layer on NCX–34 Si_3N_4 substrates gave a maximum impact energy without substrate failure of 13.6 joules. This value, while substantial, was lower than the values obtained for –200 and –325 RSSN layers and was more comparable to previously obtained results using 100% –100, +200 Si layers. The smoothness of the layer was also not as good as that obtained for either –200 or –325 RSSN layers. Thus, the mixed particle size layers were dropped from further consideration.

4.4.1.2 1370°C Ballistic Impact Testing of Fine Grained RSSN Layers

Ballistic impact tests at 1370°C were also performed on NC-132 and NCX-34 Si_3N_4 substrates with RSSN layers fabricated from both -325 and -200 Si powder. Two types of RSSN layers were investigated, one with 5 vol % residual Si and one with ~25 vol % Si. The results of these tests are given in Tables XII and XIII.

Table XII shows the RT and 1370°C ballistic impact resistance for -325 Si RSSN layers with 5 vol % residual Si on both NC-132 and NCX-34 Si_3N_4 substrates. The impact resistance of RSSN layers with 5 vol % Si on NC-132 Si_3N_4 substrates is substantially higher at 1370°C than at RT, reflecting the greater impact resistance of NC-132 Si_3N_4 at elevated temperature. The impact resistance of RSSN layers containing 5 vol % Si on NCX-34 Si_3N_4 at RT is somewhat higher than the same layers on NC-132 Si_3N_4, as expected. However, at 1370°C the impact resistance for the NCX-34 Si_3N_4/RSSN samples drops considerably, and is much inferior to NC-132 Si_3N_4/RSSN material. The fracture of the samples with NCX-34 substrates at 1370°C is rather unusual. On impact, the samples split in half in the direction normal to the hot-pressing direction. The origin of fracture is rather difficult to discern since the fracture surface is extremely flat. However, when the samples were photographed using oblique lighting, the fracture origin became discernible. Figure 16 shows a sample of NCX-34 Si_3N_4 with an RSSN layer fabricated from -325 Si with 5 vol % residual Si, that was impacted at 1370°C at a velocity of 169 m/sec (4.9 joules). The RSSN layer has, for the most part, remained strongly bonded to the substrate while the NCX-34 Si_3N_4 substrate has failed in the usual manner for this material at 1370°C. Figure 17 shows one side of the fracture surface of this sample. It appears that the fracture origin is located near a corner (i.e., the top edge) of the substrate, approximately 8 mm away from the point of impact. This type of fracture was typical for most of the NCX-34 Si_3N_4 samples impacted at 1370°C.

Table XIII gives the results of 1370°C ballistic impact tests for -325 and -200 Si RSSN layers on both NC-132 and NCX-34 Si_3N_4 substrates with ~25 vol % residual Si present in the RSSN layers. Similar to the results obtained at RT, RSSN layers of both -325 and -200 Si, on either NC-132 or NCX-34 Si_3N_4, that contain >20 vol % residual Si, result in much greater ballistic impact resistance than RSSN layers with less than 20 vol % Si. Again, as found for RSSN layers with 5 vol % Si, the samples with NC-132 substrates exhibited greater impact resistance at 1370°C than similar samples with NCX-34 Si_3N_4 substrates. The fracture origin for the NCX-34 samples was again difficult to determine. The -325 RSSN layers on NC-132 substrates gave slightly higher impact values than the -200 RSSN layers, as was noted at RT for these layers (with 20 vol % Si) on NCX-34 substrates.

A summary of all ballistic impact tests of RSSN layers on NC-132 and NCX-34 Si_3N_4 substrates is presented in bar graph form in Figs. 18 and 19, respectively. From these figures, it is immediately obvious that maximum impact resistance for any given particle size RSSN layer is only obtained when that layer contains >20 vol % unreacted Si.

18

4.4.1.3 Ballistic Impact Observations

The role of the residual Si within RSSN energy absorbing surface layers in maximizing the tolerance of the RSSN/HPSN combinations to ballistic impact of hardened chrome-steel spheres is not fully understood. It appears that the residual Si absorbs the spheres' energy and slows it as the Si is crushed, fractured, and, it appears, actually ignited by the friction caused by the impact event. Figures 20a and 20b show the impact surface of a steel ball after RT impact with a control sample of NCX-34 Si_3N_4 at a velocity of 130 m/sec (2.8 joules). This velocity is sufficient to fracture the NCX-34 Si_3N_4 sample. The steel sphere in Fig. 20 is considerably flattened and exhibits cracks that originated at the point of impact. In Fig. 20b the grinding marks from the Si_3N_4 surface can be seen imprinted on the contact area of the steel sphere.

Figures 21a and 21b show the impact surface of a steel ball after RT impact with an NCX-34 Si_3N_4 sample having a -200 RSSN surface layer with ~6 vol % residual Si. The impacting velocity was 230 m/sec (9.1 joules) which was sufficient to fracture the NCX-34 Si_3N_4 substrate. The surface of the sphere is roughened by passing through the RSSN layer and the contact area with the NCX-34 Si_3N_4 substrate is quite small. Some particles of RSSN layer appear to be adhering to the surface of the sphere.

Figures 22a and 22b show the impact surface of a steel sphere after RT impact with an NCX-34 Si_3N_4 sample having a -200 RSSN surface layer containing 21 vol % residual Si. The surface of the sphere is very abraded and roughened with no contact area with the substrate visible. Large particles of the RSSN layer appear to be imbedded in the surface and, although not apparent in this view, the impacting surface of the sphere has been slightly worn away by passing through the RSSN layer, losing ~.5 mg of weight. Figure 23 shows the impact point at the bottom of a hole created in a -200 RSSN layer by a steel sphere impacting at a velocity of 300 m/sec. Flattening of the RSSN layer near the impact point is quite evident. At the moment of impact of a steel sphere with an RSSN layer containing considerable residual Si, a flash of sparks can be seen emanating from the impact point. These sparks are apparently ignited Si particles caused by frictional heating during the impact event. The striations seen on the RSSN surface in Fig. 23 are evidently caused by the outward passage of these particles. Whatever the actual mechanism, the Si particles in the RSSN layer definitely tend to slow down the incoming steel sphere to a greater extent than RSSN layers with little or no residual Si.

Another important observation concerning the RSSN energy absorbing surface layer concept is that, while most of the RSSN/HPSN combinations tested in ballistic impact had RSSN layers of 1 mm thickness, a substantial amount of energy can be absorbed by much thinner layers, as shown in Table XIV. Even a 0.25 mm thick RSSN layer absorbs 4 times the amount of energy of an NC-132 Si_3N_4 substrate with no layer. This is important due to the fact that some components could be too small to accommodate a standard RSSN layer of 1 mm thickness.

19

4.4.2 4-Pt Bend Testing of RSSN/HPSN Combinations

From previous work on energy absorbing RSSN surface layers on NC-132 Si_3N_4 (Ref. 10), it had been shown that a severe strength degradation occurred when the RSSN/HPSN sample was tested in either Charpy impact or bending with the RSSN side in tension. In order to determine at what point in the nitriding cycle the strength degradation at the RSSN/HPSN interface occurs, a series of nitriding runs were done under differing conditions, using both -325 Si and -100, +200 Si powder layers on NC-132 and NCX-34 substrates. Sets of Si_3N_4 bend samples (4.44 x 0.508 x 0.254 cm) with the two different Si powder layers were subjected to four different cycles: (1) Ar, $1150^{\circ}C$, 20 hrs; (2) Ar, $1150^{\circ}C$, 20 hrs, plus N_2, $1250^{\circ}C$, 24 hrs; (3) Ar, $1150^{\circ}C$, 20 hrs, plus N_2, $1250^{\circ}C$, 24 hrs, plus N_2, $1375^{\circ}C$, 24 hrs; and (4) the normal nitriding cycle of 20 hrs in Ar at $1150^{\circ}C$, 24 hrs in N_2 at $1250^{\circ}C$, followed by 60 hrs in N_2 at $1375^{\circ}C$. The samples were then tested in 4-pt bending at RT with the RSSN (or Si) layer in tension.

The results of these tests are given in Table XV. It is apparent that degradation of the sample strength does not occur until the nitriding temperature of $1375^{\circ}C$ is reached. A nitriding time of 24 hrs at this temperature is sufficient to degrade the strength of nitrided NC-132 and NCX-34 Si_3N_4 samples with -325 mesh Si layers to half the control value, with longer times being necessary to achieve this with the coarser -100, +200 mesh Si layers. Note that NC-132 Si_3N_4 by itself appears to increase somewhat in strength after undergoing the standard nitriding cycle, while the NCX-34 Si_3N_4 is decreased in strength somewhat. The intermediate temperature strength degradation problem of this lot of NCX-34 Si_3N_4 may be contributing to the loss in strength, even though the nitriding treatment is carried out in a nonoxidizing environment.

An X-ray diffraction analysis of the nitrided -325 Si layers after 24 hrs at $1250^{\circ}C$ in N_2 indicates that the layer consists primarily of Si, with only about 10 vol % of the Si converted to Si_3N_4. In contrast, the samples nitrided to $1375^{\circ}C$ for 24 hrs exhibited over 90 vol % conversion to a mixture of α and β Si_3N_4. It thus appears that as soon as a substantial amount of the Si powder layer reacts with the N_2 to form Si_3N_4, either the surface of the Si_3N_4 substrate becomes a source of stress concentrating flaws due to interaction with the nitrided Si grains, or that the interfacial bonding is increased to the point that cracks propagating through the RSSN layer during stressing are not blunted or deflected at the RSSN/HPSN interface but continue to propagate into the HPSN.

20

The fracture surfaces of -325 Si layers on NC-132 Si_3N_4 nitrided at maximum temperatures of 1250°C and 1375°C for 24 hrs were examined by scanning electron microscopy (SEM). The 1250°C nitrided sample is shown in Fig. 24. This particular sample had a 4-pt bend strength of 586 MPa (85 ksi) which is somewhat less than the control value of 662 MPa (96 ksi). The fracture surface is fairly rough with the fracture origin located near the sample edge. The origin is indicated by arrows in Fig. 24 and appears to be a small void within the NC-132 Si_3N_4 at a distance of ~20μ from the tensile surface. The nitrided Si surface layer does not appear to have influenced the fracture of this sample and actually has debonded from the NC-132 Si_3N_4 near the fracture origin.

Figure 25 shows the fracture surface of the -325 Si sample nitrided at 1375°C for 24 hrs. The nitrided Si layer is primarily converted to Si_3N_4 and is quite strongly bonded to the NC-132 Si_3N_4. The fracture surface of the NC-132 Si_3N_4 is very smooth, which is indicative of a sample with low bend strength; in this case 300 MPa (44 ksi). The fracture origin is indicated by arrows in Fig. 25 and appears to be a void of about 20μ diameter in the RSSN layer located about 50μ from the NC-132 Si_3N_4 interface. This particular sample appears to have had a few very large bubbles (i.e. voids) in the RSSN layer but they do not appear to affect the nature of fracture. Other -325 Si layers, nitrided at 1375°C, containing no large voids exhibit the same type of fracture behavior.

Some RSSN/HPSN combinations were rather difficult to fabricate with a well bonded interface, in particular the -325 RSSN layers on NCX-34 Si_3N_4 substrates. A typical fracture surface for a weakly bonded -325 RSSN layer on NCX-34 Si_3N_4 is shown in Fig. 26. The RSSN layer on this sample is still adhered to the substrate; many -325 RSSN layers debonded when the samples were broken. The relatively rough surface of the NCX-34 substrate cross section is indicative of a strong sample, in this case 702 MPa (102 ksi). Figure 27, by way of contrast, shows the quite smooth fracture surface of the substrate for a -100, +200 RSSN layer on NCX-34 Si_3N_4 with a degraded strength of only 407 MPa (59.1 ksi). In this case, the fracture origin appears to be located at some point within the RSSN layer, near the interface.

In order to determine whether or not the strength degradation is due to interaction between the Si particles and the Si_3N_4 substrate during nitriding, NCX-34 Si_3N_4 samples that had both -325 Si and -100, +200 Si powder lightly sprinkled on the tensile surface were nitrided by the usual method. These samples, when tested at RT with the lightly covered RSSN surface in tension, exhibited significant degradation in strength. The fracture origin was always located on the surface at either a nitrided particle of Si or a depression that at one time was associated with a nitrided Si particle. Figure 28 shows a typical fracture origin for a sample with a surface covered with nitrided -100, +200 Si particles.

21

4.4.2.1 Bend Test of RSSN/HPSN Combinations Nitrided in a N_2/H_2 Mixture

In order to insure that impurities in the Si powder or oxygen contamination from the nitriding gas are not contributing to the observed degradation, additional nitriding runs were done using a much purer Si starting powder and using a 96% N_2-4% H_2 mixture as the nitriding media. Both NC-132 and NCX-34 Si_3N_4 bend specimens were fabricated with approximately one mm thick layers of -100, +200 Si and -325 Si powder of two purities; a nominal 98% pure powder that has been used throughout this program and a high purity 99.6% powder. The chemical analyses of these powders was given previously in Table III. It can be seen that the main impurities in the -325 (99.6%) powder are Al and Pb (.1%) while the -325 (98%) powder contains Fe (.7%), Al (.2%), Mn (.3%), Cr (.1%), and Ca (.1%). The samples were nitrided according to the standard schedule except that the nitriding atmosphere consisted of 96% N_2/4% H_2, instead of the usual 100% N_2.

The results of RT 4-pt bend strength tests with the RSSN in tension are given in Table XVI. It can be seen that both NCX-34 and NC-132 Si_3N_4 with well bonded RSSN layers of 98% purity -325 Si are not significantly degraded in strength when the nitriding is carried out in a N_2/H_2 mixture. The 99.6% -325 Si and the -100, +200 Si of 98.5% purity, when nitrided using N_2/H_2 mixtures on both NC-132 and NCX-34 Si_3N_4 substrates, do tend to degrade the strength; although less so for the NCX-34 Si_3N_4. For some reason, the -325 Si (99.6%) layers on NCX-34 Si_3N_4 usually exhibit rather poor bonding. This may be due to the very small particle size, i.e. high surface area, of this powder causing debonding due to high shrinkage during drying of the Si layer. Figures 29 and 30 show the fracture surfaces of the -325 (98%) Si RSSN layers on NC-132 and NCX-34 Si_3N_4, respectively. The RSSN layers on both samples are very well bonded to the substrate and the fracture surfaces are quite rough, in agreement with the high strength of these samples. Shown in Fig. 31 is the usual fracture surface obtained when -325 Si (98%) layers on NC-132 Si_3N_4 are nitrided to 1375°C, 60 hrs, in pure N_2. This sample exhibited a bend strength of 264 MPa (38.3 ksi) compared to 659 MPa (95.6 ksi) for the sample in Fig. 29 nitrided in 96% N_2/4% H_2. The fracture origin for the samples nitrided in N_2/H_2 mixtures appears to be at or very near the RSSN/HPSN interface; near the right corner for the sample in Fig. 29 and midway between the left corner and center for the sample in Fig. 30. The fracture origin for the degraded sample in Fig. 31 is not readily apparent, but appears to be within the RSSN layer.

Subsequent 4-pt bend tests have been done on samples of both NC-132 and NCX-34 Si_3N_4 with -325 and -200 Si layers, that were nitrided in N_2/H_2 mixtures along with ballistic impact samples. Three bend test samples of each RSSN/HPSN combination were included in each nitriding run. All of the samples nitrided in the 96% N_2/4% H_2 mixture showed some degradation in bend strength. The NCX-34 Si_3N_4 samples with either -325 or -200 RSSN layers containing 20-25 vol % Si

22

gave bend strengths that averaged 572 MPa (83 ksi). The NC-132 Si_3N_4 samples with similar RSSN layers averaged 503 MPa (73 ksi). These results are also given in Table XVI. This represents a 32% drop in strength for the NCX-34 Si_3N_4 and a 24% drop in strength for the NC-132 Si_3N_4 over the as-received condition. However, the NCX-34 Si_3N_4 degrades ~15% in strength due to the nitriding treatment alone. This drop in strength may be connected to the observed intermediate temperature oxidation problem of this NCX-34 Si_3N_4 material. Figures 32 and 33 show all of the 4-pt bend strength data for NC-132 and NCX-34 substrates, respectively, with the various RSSN layers, plotted in bar graph form.

4.4.2.2 Conclusions on the Degradation of RSSN/HPSN Bend Strength

In general, when well-bonded RSSN layers on HPSN substrates are tested at RT in bending with the RSSN layer in tension, severe strength degradation (~50%) occurs for those samples nitrided in 100% N_2 while only moderate to very little strength degradation occurs for those samples nitrided in 96% N_2/4% H_2. Also, the strength retention is usually best for NCX-34 Si_3N_4 over NC-132 Si_3N_4, reflecting the higher initial strength of the NCX-34 material.

The reason for the strength degradation for those samples nitrided in 100% N_2 appears to be caused by the type of microstructure developed within the RSSN layer and the way it bonds to the HPSN substrate. RSSN nitrided in flowing $N2$ is comprised primarily of large particles of β-Si_3N_4, with very little α-Si_3N_4 whisker formation between the β-Si_3N_4 particles, as discussed by Lindley, et al (Ref. 14). Bonding in this type of RSSN layer on a HPSN substrate consists primarily of direct β-Si_3N_4 to β-Si_3N_4 particle bonding and β-Si_3N_4 particle to HPSN substrate surface (also β-Si_3N_4) bonding. From experiments with sprinkled Si powder nitrided in 100% N_2 on HPSN substrates, it was found that the nitrided Si particles bond very strongly to the substrate with a continuous β-Si_3N_4 structure and act as large surface flaws, causing strength degradation. RSSN layers on HPSN substrates, nitrided in pure N_2, cause strength degradation by allowing crack propagation to occur through the direct β-Si_3N_4 to β-Si_3N_4 particle bonding and then on through the HPSN substrate. The fact that most well-bonded RSSN/HPSN combinations, nitrided in pure N_2, do not exhibit fracture origins at the RSSN/HPSN interface but rather somewhere in the RSSN layer indicates that flaws (i.e. porosity) in the RSSN structure are controlling the mode of fracture.

RSSN layers nitrided in N_2/H_2 mixtures exhibit a much different microstructure than those nitrided in pure N_2. Every β-Si_3N_4 particle, whether or not it contains residual Si in the center, is surrounded by a fine structure of α-Si_3N_4 whiskers. This α-Si_3N_4 whisker mesh separates the β-Si_3N_4 grains from each other and from the HPSN substructure, thus not allowing a direct path for crack propagation. The flaw size within the RSSN nitrided in N_2/H_2 mixtures is also considerably reduced, due to the pores between Si particles becoming filled with the fine α-Si_3N_4 structure. Well bonded RSSN layers on HPSN substrates always exhibit fracture origins at the RSSN/HPSN interface, indicating

23

that the fracture mode is controlled by flaws at the interface, not within the RSSN layer as is the case when nitriding is done in pure N_2. And, since the interface consists primarily of α-Si_3N_4 whiskers bonded to the HPSN substrate, the flaws at the interface are not large, thus leading to minimal strength degradation.

4.4.3 Task I - Conclusions

The general goal of Task I of this program was to develop RSSN energy absorbing surface layers on hot-pressed Si_3N_4 that would consistently result in ballistic impact strengths at RT and 1370°C of over 7 ft-lbs (9.5 joules) while minimizing the RSSN/HPSN interfacial strength degradation that occurs as a result of the nitriding process. This goal has been accomplished with the development of RSSN layers of either -325 Si or -200 Si nitrided in a 96% N_2/4% H_2 mixture, to minimize interfacial strength degradation, according to a schedule that results in at least 20 vol % residual Si remaining in the RSSN layer. Using either NC-132 or NCX-34 Si_3N_4 substrates in combination with these RSSN layers meets the 7 ft-lb (9.5 joule) goal at both RT and 1370°C, with the NCX-34 Si_3N_4 material performing better at RT and the NC-132 Si_3N_4 material performing better at 1370°C. The latter observation is undoubtedly due to the higher fracture toughness of Si_3N_4 (Y_2O_3) materials at RT and the greater plastic flow at the grain boundaries of Si_3N_4 (MgO) materials at elevated temperatures.

4.5 Task II - Effect of Thermal Exposures on RSSN/HPSN Combinations With and Without Overlayers of CVD Si_3N_4

The purpose of Task II of this program is to evaluate the effect of thermal cycling to 1200 and 1370°C in air on the integrity of the RSSN/HPSN combinations, in particular the effect of silica formation within the RSSN layer on its ability to absorb energy during ballistic impact. In addition, the hot gas erosion characteristics of the RSSN layers at 1200 and 1370°C in a Mach 0.8 gas stream are to be evaluated, both with and without a thin overlayer of chemically vapor deposited (CVD) Si_3N_4. The CVD Si_3N_4 overlayer is being investigated as a possible oxidation and erosion resistant barrier for the RSSN/HPSN combinations.

4.5.1 Thermal Cycling of Si_3N_4 Control Samples

Ballistic impact samples of both NC-132 and NCX-34 Si_3N_4 were subjected to 75 thermal cycles between ~150 to 1200°C and ~200 to 1370°C in air. An exposure cycle consisted of heating to either 1200 or 1370°C in ~15 min, holding at temperature for 40 min, and then cooling to the minimum temperature in a cold air blast for 10 min. After thermal cycling, the samples were inspected visually and analyzed for weight gain and, by X-ray diffraction, for the formation of surface oxide phases. They were then tested in ballistic impact at a sample temperature of 20 and 1370°C.

24

The weight gain and oxide formation data for the thermally cycled ballistic impact control samples of NC-132 and NCX-34 Si_3N_4 are given in Table XVII. For both temperatures, the oxide layer formed on the NC-132 Si_3N_4 was much thicker than that formed on the NCX-34 Si_3N_4, as expected from previous oxidation data for these two materials. Figure 34 shows the surface of the NCX-34 Si_3N_4 (left) and the NC-132 Si_3N_4 (right) samples after the 75 cycle, 1370^oC exposure. There was no evidence of the low temperature oxidation problem previously noted for the NCX-34 Si_3N_4 occurring during cycling of this material to either 1200 or 1370^oC. The weight gain for the NC-132 Si_3N_4 was approximately three times that of the NCX-34 Si_3N_4 at 1370^oC and approximately 70% higher at 1200^oC. At 1370^oC, the oxide formed on the NCX-34 Si_3N_4 was entirely crystalline, as determined from X-ray analysis, consisting of elongated $Y_2Si_2O_7$ crystals with a small amount of SiO_2 (cristobalite). The oxide layer formed on the NC-132 Si_3N_4 was a mixture of a glassy silicate phase, SiO_2 (cristobalite), and $MgSiO_3$ (clinoenstatite). At 1200^oC, the predominant surface oxide phase formed on both materials was SiO_2 (cristobalite) with small amounts of what appears to be the X_1 phase of Y_2SiO_5 forming on the NCX-34 and small amounts of Si_2N_2O plus an unidentified phase on the NC-132 Si_3N_4.

The results of ballistic impact tests at RT and 1370^oC on thermally cycled Si_3N_4 substrates control samples are given in Table XVIII and compared to values for as-received controls. Within statistical scatter, there does not appear to be any significant effect of thermal cycling on the ballistic impact properties of either NC-132 or NCX-34 Si_3N_4. Both materials exhibit somewhat better RT ballistic impact properties and somewhat poorer 1370^oC impact properties after thermal cycling, except for the NCX-34 material cycled to 1200^oC and tested at 1370^oC. In general, the 1200^oC cycling gives higher ballistic impact results than the 1370^oC cycle, for both NC-132 and NCX-34 Si_3N_4. The fracture mode for the materials was not changed by the thermal cycling exposure.

4.5.2 Thermal Cycling of RSSN/HPSN Combinations

Samples of both NC-132 and NCX-34 Si_3N_4 with -200 RSSN layers containing ~25 vol % Si were subjected to thermal cycling tests between 150 and 1200^oC and between 200 and 1370^oC. Samples of NC-132 with -325 RSSN layers have also been thermally cycled. From weight gain measurements of cycled samples, it was determined that the -200 RSSN layers cycled 75 times to 1200^oC gained ~115 mg while the -325 RSSN layers gained ~110 mg. The -200 RSSN layers cycled to 1370^oC gained ~150 mg while the -325 RSSN layers gained ~130 mg. No difference in weight gain was noted between RSSN layers on NC-132 or NCX-34 substrates. X-ray analysis of the cycled RSSN layers revealed that the oxide product consisted entirely of α-cristobalite (SiO_2). The amount of residual Si in the cycled layers was essentially unchanged as calculated from X-ray analysis, so that the silica that was formed resulted from the reaction of oxygen with the

α and β Si_3N_4, not with the Si. This would be expected, since the residual Si exists in the interior of β-Si_3N_4 particles. Photomicrographs of the cycled RSSN layers revealed that the silica almost completely filled the void space that previously existed between Si_3N_4 particles, as shown in Fig. 35 for a -200 RSSN layer cycled 75 times to $1370^{\circ}C$. At high magnifications, as shown in Fig. 35b, it can be seen that the Si particles appear to be oxidizing somewhat along grain boundaries.

The results of RT and $1370^{\circ}C$ ballistic impact rests on the RSSN/HPSN combinations, both as-fabricated and cycled 75 times to $1200^{\circ}C$ and $1370^{\circ}C$ are shown in Table XIX. Only the energy and velocity necessary to fracture the hot-pressed substrate are shown in Table XIX. From these results, it can be seen that the ballistic impact resistance of -200 Si RSSN layers on both NC-132 and NCX-34 Si_3N_4 substrates, tested either at RT or $1370^{\circ}C$, either increases or stays the same after 75 thermal cycles to $1200^{\circ}C$ or $1370^{\circ}C$. The -325 RSSN layers on NC-132 Si_3N_4 also showed no decrease in RT impact resistance after thermal cycling.

From the tests conducted on samples cycled to either 1200 or $1370^{\circ}C$, it is apparent that the formation of α-cristobalite in the interior and on the surface of the porous RSSN layers does not cause degradation of the RSSN layer and in most instances has a beneficial effect on its impact resistance. The silica forms predominantly at the expense of the Si_3N_4, not the residual Si, and thus does not reduce the amount of residual Si below the apparently critical value of 20 vol % necessary for optimum impact resistance. The silica also appears to withstand the high to low cristobalite transformation that occurs when the sample is cooled through the $200-275^{\circ}C$ range, at least without cracking or delaminating the RSSN layer.

4.5.3 Thermal Cycling of RSSN/HPSN Combinations with CVD Si_3N_4 or SiC Overlayers

As described in the following section on Mach 0.8 gas erosion testing, the formation of a protective CVD Si_3N_4 overlayer on the RSSN layers was not possible due to the residual Si present in the optimized RSSN layers interfering with the deposition process at the usual deposition temperatures of $1400-1450^{\circ}C$. A fully nitrided RSSN layer was shown to be amenable to CVD Si_3N_4 deposition at $1450^{\circ}C$ with subsequent thermal cycling of the sample to $1370^{\circ}C$ showing no appreciable oxidation of the RSSN layer. However, the impact resistance of the fully nitrided RSSN layers is about one-third of layers with 20 vol % residual Si so that if oxidation protection of the RSSN layer by a CVD Si_3N_4 overlayer is desired, a compromise in impact resistance must be made.

26

Since CVD SiC can be deposited at a much lower temperature than CVD Si_3N_4, it was decided to investigate RSSN layers with overlayers of CVD SiC. Even though the thermal expansion coefficient of SiC ($\sim 4.5 \times 10^{-6}/^{\circ}$C) is somewhat higher than that of Si_3N_4 ($\sim 3.1 \times 10^{-6}/^{\circ}$C), thus causing residual tensile stresses in the SiC upon cooling from the deposition temperature (1120°C), it was thought that a very thin but continuous CVD SiC overlayer could be protective of the RSSN layers.

CVD SiC deposition was carried out at 1120°C using a mixture of methane and hydrogen saturated with methyldichlorosilane. The first samples of NC-132 with -200 Si layers were coated with CVD SiC of $\sim$6 mils (.15 mm) in thickness. On cooling from deposition, the CVD SiC coatings cracked but were still very adherent to the RSSN layer. The corncob appearance of the CVD SiC and the cracks formed can be seen in Fig. 36. Upon thermal cycling to 1370°C, the SiC overlayer tended to spall off, thus not offering any protection from oxidation. The sample shown in Fig. 37 completed 21 cycles to 1370°C with the coating starting to spall after $\sim$10 cycles. Due to the spallation of the coating, no weight gain data could be taken but it can be assumed that the RSSN layer contained considerable silica.

The CVD deposition parameters were changed to obtain a thinner, finer grained SiC coating. Subsequent samples exhibited coatings of 0.5 to 1.5 mils (12-36μ) in thickness. Figure 38 shows the CVD SiC surface of a sample of NC-132 with -200 RSSN layer, with the thickness of the CVD SiC coating being $\sim$1 mil (25μ). As can be seen in this figure, cracks are still in evidence in some areas of the coating. It was found that all coatings of thickness 1 mil (25μ) or greater contained cracks, whereas thinner SiC coatings were crack free.

A total of ten NC-132 ballistic impact samples with -200 RSSN layers (20% Si) were coated with 0.5-1.5 mils (12-36μ) of CVD SiC and then subjected to 75 thermal cycles to 1370°C. These samples along with nonthermal cycled samples with CVD SiC overlayers, were then tested at RT and 1370°C in ballistic impact. The weight gain and oxide formation data for the thermally cycled samples is shown in Table XX. As can be seen from Table XX, the weight gain of the samples with CVD SiC overlayers is somewhat higher than NC-132 Si_3N_4 substrates and substantially lower than the RSSN/HPSN combinations with no CVD SiC overlayer. The actual values of weight gain for the samples with CVD SiC overlayers ranged from 36 mg for thin ($\sim$12μ) CVD SiC, with no cracks evident, to 70 mg for a thicker ($\sim$36μ) CVD SiC that exhibited cracking similar to that shown in Fig. 38. A fairly thick silica layer formed on the CVD SiC during cycling which, on cooling, exhibited some cracking as shown in Fig. 39. From the weight gain data and from X-ray diffraction analysis it is apparent that while some internal oxidation of the RSSN layer is occurring, it is much reduced by the presence of the CVD SiC overlayer.

The ballistic impact resistance of as-fabricated and thermally cycled samples with CVD SiC overlayers was determined at RT and 1370°C, is shown in Table XXI. The only difference noted between those samples with CVD SiC coatings and those without was a slightly lower impact resistance for the thermally cycled samples with CVD overlayers. This is likely due to the relatively lesser amount of internal oxidation within the RSSN layer for the samples with CVD SiC overlayers. Table XXII summarizes all of the ballistic impact data obtained on thermally cycled samples, both with and without CVD SiC overlayers.

4.5.4 Mach 0.8 Hot Gas Erosion Testing

In order to determine the effect of a simulated gas turbine environment on the erosion and oxidation characteristics of the RSSN energy absorbing surface layers, samples of NC-132 and NCX-34 Si_3N_4, both with and without -200 and -325 RSSN layers, were subjected to Mach 0.8 hot gas erosion testing for 5 hrs at sample surface temperatures of 1200 and 1370°C. The samples tested at 1200°C were approximately 1.92 x 1.23 x 0.64 cm (0.75 x 0.50 x 0.25 in) in size with the largest face positioned at a 30° angle to the direction of hot gas flow. Samples run at 1370°C had a substrate thickness of 0.28 cm (0.15 in). Sample temperatures were monitored by a continually recording optical pyrometer. Samples of -325 and -200 RSSN layers with CVD Si_3N_4 or SiC overlayers were also tested in erosion at 1200 and 1370°C.

4.5.4.1 Erosion Testing of Si_3N_4 Controls

Both NC-132 and NCX-34 Si_3N_4 controls were tested in erosion at 1200 and 1370°C. The two control samples of hot-pressed Si_3N_4 tested at 1200°C did not exhibit any detectable weight change or surface recession. X-ray analysis of the exposed surfaces indicated no detectable oxide formation during the 5 hr test. Erosion testing at 1370°C for 5 hrs on NC-132 and NCX-34 Si_3N_4 controls, however, did produce measurable surface recession. Somewhat surprisingly, the NCX-34 Si_3N_4 sample eroded considerably more (~25μ) than the NC-132 Si_3N_4 (~2.5μ). The NC-132 Si_3N_4 sample gained a slight amount of weight (0.1 mg) while the NCX-34 Si_3N_4 sample lost weight (3.5 mg). Both samples exhibited a very thin oxide scale on the surface (predominantly α-cristobalite from X-ray diffraction measurements) which would tend to increase the weight of the sample; however, in the case of the NCX-34 Si_3N_4 this weight gain was more than offset by weight loss due to material erosion. Figures 40 and 41 show the eroded surfaces of the NC-132 and NCX-34 samples tested at 1370°C. While both samples exhibit a rather rough oxidized surface, the NC-132 appears to have a glassy, bubbly oxide layer while the NCX-34 has a more crystalline but substantially rougher surface.

4.5.4.2 Erosion Testing of RSSN/HPSN Combinations

Samples of NC-132 and NCX-34 Si_3N_4 with -200 and -325 RSSN layers, containing ~25 vol % Si, were erosion tested for 5 hrs at 1200 and 1370°C. The RSSN layers tested at 1200°C did not exhibit measurable surface recession, but did exhibit substantial weight gains of ~20 mg. RSSN samples tested at 1370°C exhibited a slight amount of surface recession (~8μ) (Fig. 42) but a somewhat lower weight gain of ~12 mg; the latter due to less of the substrate surface being covered with the RSSN layer. From X-ray analysis, a substantial amount of SiO_2 (α-cristobalite) was present on the surface and in the interior of the RSSN layers tested at both 1200 and 1370°C. Figure 43 shows the -325 and -200 RSSN layers tested at 1370°C, along with the NC-132 and NCX-34 Si_3N_4 controls tested at the same temperature. No difference in erosion behavior between the -325 and -200 RSSN layers can be observed. Figure 44 shows the erosion surface of the -200 RSSN layers tested at 1200 and 1370°C, with the 1370°C sample exhibiting a much rougher surface oxide scale. Table XXIII gives the complete results of the Mach 0.8 hot gas erosion tests on the Si_3N_4 controls and RSSN layers.

4.5.4.3 Erosion Testing of RSSN Layers with CVD Si_3N_4 and SiC Overlayers

While the hot gas erosion resistance of RSSN layers containing 25 vol % Si at 1200 and 1370°C is quite good, as far as surface recession is concerned, the large amount of oxide formation may be detrimental during very long time exposures. It would thus be desirable to have a CVD coating system that would protect the RSSN layer from oxidation. CVD Si_3N_4 coatings deposited at the usual deposition temperatures of 1400-1450°C, using a mixture of SiF_4 + NH_3, can be extremely protective of fully nitrided RSSN material; however, the presence of residual Si for optimum impact resistance in the RSSN layers studied under this program has prevented the formation of a successful CVD Si_3N_4 coating applied at 1400-1450°C.

A sample of NCX-34 Si_3N_4 with a -200 RSSN layer that had been coated with a .005 cm (2 mil) layer of CVD Si_3N_4 at a deposition temperature of 1450°C (Fig. 45), was run for 5 hrs in the hot gas erosion rig at 1200°C. The sample exhibited no surface recession after the run, but did gain a considerable amount of weight (22 mg), indicating that the CVD Si_3N_4 layer did not completely cover the RSSN surface. X-ray analysis indicated that the CVD Si_3N_4 layer was 100% α-Si_3N_4, both before and after erosion testing. From optical microscope examination, this coating covered the RSSN quite well except for occasional pinholes. The pinholes appeared to be forming over residual Si particles in the RSSN layer. It was apparent that the residual Si was melting and/or vaporizing during the CVD process and preventing complete coverage of the RSSN surface.

The CVD process parameters were changed such that the chamber temperature would not exceed 1400°C, thus preventing Si meltout. The CVD Si_3N_4 coating formed under these conditions appeared to be continuous when viewed in cross-section (Fig. 46), but still contained a few pinholes located over residual Si particles. While the Si did not appear to be melting, the Si vapor pressure must be high enough to cause Si vaporization, thus preventing complete Si_3N_4 deposition. A sample of NC-132 Si_3N_4 with a -325 RSSN layer, covered with a CVD Si_3N_4 coating of 2 mils (50μ) that was deposited at 1400°C, was run for 5 hrs at 1370°C in the hot gas erosion rig. The sample gained a considerable amount of weight (33 mg), indicating that oxygen was penetrating into the RSSN layer through pinholes in the CVD coating, but exhibited no measurable surface recession and no oxide formation on the CVD Si_3N_4 surface. It is apparent that the erosion resistance of an RSSN layer with a CVD Si_3N_4 coating would be excellent if a pinhole-free coating could be deposited.

Since a protective CVD Si_3N_4 overlayer could not be obtained, CVD SiC layers were deposited at 1120°C on erosion samples of NC-132 and NCX-34 with -200 RSSN layers. The CVD SiC layers were ~1.5 mils (36μ) in thickness. The results of erosion tests at 1200 and 1370°C (see Table XXIII) showed that these overlayers were very resistant to surface recession and relatively good in oxidation protection. Compared to the CVD Si_3N_4 overlayers, the CVD SiC overlayed samples gained only 6 mg (vs 22 mg for Si_3N_4) at 1200°C and only 2.5 mg (vs 33 mg) at 1370°C. The slight amount of SiO_2 that formed on the surface of the CVD SiC at 1370°C was evidently sealing the surface cracks in the SiC, thus not allowing significant internal oxidation of the RSSN layer to occur. Figure 47 shows the cross-section of a -200 RSSN layer with a CVD SiC overlayer both before and after a 5 hr, 1370°C erosion test. The erosion test has roughened the CVD SiC overlayer somewhat, but other wise there exists no significant difference in the two samples.

Interestingly, a rather dense transition zone exists under the CVD SiC overlayer and can be seen in both samples in Fig. 47. From electron microprobe examination, this transition zone consists of residual Si particles surrounded by a rather dense matrix that contains Si, N, C, and some O. The reactant gases during the early stages of the CVD process are evidently reacting with the α-Si_3N_4 whisker matrix forming either a mixture of SiC and Si_3N_4 with some O_2 contamination or some compound of the four elements. If a compound is forming, X-ray analysis has not been able to identify it.

Bend tests conducted on as-nitrided -200 RSSN layers on NCX-34 Si_3N_4 and identical samples after the application of a CVD SiC overlayer showed a decrease in RT 4-pt bend strength for the samples with CVD SiC overlayers compared to those without. The samples without CVD SiC overlayers averaged 590 MPa (86 ksi) when the -200 RSSN layer was tested in tension, while those with CVD SiC

overlayers averaged 421 MPa (61 ksi). The fracture origin of the samples with
CVD SiC overlayers was invariably located close to the RSSN/HPSN interface near the
corner of the sample where the dense CVD SiC/RSSN transition zone came in-
to contact with the HPSN substrate, as shown in Fig. 48. The dense transition
zone is evidently providing a crack path at the corners of the sample where it
is in contact with the HPSN substrate. Samples tested that had 0.25 mm (10
mils) ground off each side so as to remove the transition zone that is in con-
tact with the HPSN substrate did not exhibit severe strength degradation,
averaging 540 MPa (78 ksi) in strength.

In an actual component of dense Si_3N_4 with an RSSN energy absorbing sur-
face layer overlaid by a CVD SiC coating, it would be likely that the CVD SiC/
RSSN transition zone would not come into contact with the dense Si_3N_4 component.
If it did, the part could probably be designed so that the transition zone
region in contact with the dense Si_3N_4 would not be a highly stressed area.

V. CONCLUSIONS

The major conclusions that can be reached from work done on this program to improve the toughness (impact resistance) of hot-pressed Si_3N_4 are as follows:

1. The ballistic impact resistance and bend strength at RT of Norton Co. NCX-34 hot-pressed Si_3N_4 is substantially higher than that of NC-132 Si_3N_4. At $1370^{\circ}C$ the ballistic impact resistance of the two materials is approximately equal.

2. Certain lots of NCX-34 Si_3N_4 with Y_2O_3 additive, including all three billets used for this program, exhibit catastrophic oxidation properties in the temperature range of $700-1000^{\circ}C$. The cause of this phenomenon is not fully understood and must be further investigated in order to fully utilize the potential of Si_3N_4 with Y_2O_3 additive.

3. Reaction sintered Si_3N_4 (RSSN) surface layers on either NC-132 or NCX-34 Si_3N_4 substrates cause a severe (~50%) drop in strength of the substrate when the nitriding is carried out in pure flowing N_2, but only a minimal drop in strength when the Si powder layer is nitrided in a 96% N_2/4% H_2 mixture. The reason for the strength degradation appears to be connected with the difference in microstructure between RSSN layers nitrided in pure N_2 and in N_2/H_2 mixtures. Large, interconnected $\beta-Si_3N_4$ particles are formed when nitriding is done in pure N_2 whereas the $\beta-Si_3N_4$ particles formed in N_2/H_2 mixtures are always separated from each other and from the substrate by an $\alpha-Si_3N_4$ whisker mat. Thus, no large stress-concentrating flaws ($\beta-Si_3N_4$ particles) are bonded directly to the HPSN surface and cracks initiating in the RSSN layer cannot propagate directly through $\beta-Si_3N_4$ grains and into the HPSN substrate.

4. Ballistic impact tests at RT and $1370^{\circ}C$ on NC-132 and NCX-34 Si_3N_4 substrates with 1 mm thick RSSN layers fabricated from either -325 mesh, -200 mesh, or -100, +200 mesh Si powder indicated that fully nitrided layers (i.e., no residual Si) result in only modest (50-100%) improvement in impact resistance over HPSN control values.

5. To obtain optimum impact resistance on the order to 600-700% improvement over control values, the nitriding schedule must result in at least 20 vol % residual Si remaining within the RSSN layer. The residual Si is apparently absorbing a great deal of energy as it is crushed and fractured by the ballistic projectile.

6. For a smooth surface finish and a relatively dense (~30% porosity) microstructure, either -325 or -200 mesh Si powder nitrided in N_2/H_2 mixtures to a residual Si content of 20-25 vol % is preferred over the rather coarse -100, +200 Si powder previously used. Control of the residual Si content with the finer powders is more difficult, however.

7. Thermal cycling 75 times between 150-200°C to either 1200 or 1370°C does not adversely affect the ballistic impact resistance of either NC-132 or NCX-34 Si_3N_4 control samples nor does it affect the impact improvement of -325 and -200 RSSN layers (25 vol % Si) on HPSN substrates. A large amount of silica (cristobalite) is formed within the RSSN layers during cycling, but this did not affect the RSSN/HPSN bonding or the ability of the RSSN layers to absorb energy during impact since the silica forms primarily at the expense of the α-Si_3N_4 within the RSSN layers and thus does not reduce the Si content below the critical 20 vol % level.

8. Attempts to form an oxidation and erosion protective CVD Si_3N_4 over-layer on RSSN layers containing residual Si were not successful due to the high Si vapor pressure at the deposition temperature (1400-1450°C) interfering with the deposition process and causing pinhole formation over residual Si particles.

9. CVD SiC overlayers were successfully deposited at 1120°C on RSSN layers containing Si and, while cracking of the SiC was often a problem, crack-free coatings were deposited and, on thermal cycling to 1370°C, did offer substantial oxidation protection and no decrease in ballistic impact properties, although a bend strength decrease was noted due to crack propagation through a dense transition zone under the CVD SiC coating.

10. Mach 0.8, 5 hr, hot gas erosion testing at sample temperatures of 1200°C and 1370°C on NC-132 and NCX-34 Si_3N_4 controls showed that no surface recession or weight change occurred at 1200°C, while at 1370°C a very slight surface recession (2.5μ) and weight gain (+0.1 mg) was observed for NC-132 Si_3N_4 and a rather large surface recession (25μ) and weight loss (-3.5 mg) for NCX-34 Si_3N_4. For the -325 and -200 RSSN layers with 25 vol % Si, no surface recession was detected at 1200°C while a small surface recession (~8μ) was detected at 1370°C. A substantial weight gain was observed at both temperatures due to internal oxidation of the RSSN layer.

11. Erosion tests of -200 RSSN layers (25 vol % Si) with 36μ (1.5 mil) overlayers of CVD SiC showed no surface recession at 1200 or 1370°C and very small weight gains. It is felt that an optimized CVD SiC overlayer could offer excellent oxidation and erosion protection for RSSN energy absorbing surface layers on dense Si_3N_4 substrates.

12. From the results of various research programs carried out during the past six years that have been concerned with improving the impact resistance of Si_3N_4 through the use of compressive surface layers (Refs. 4-6) or energy absorbing surface layers (Refs. 1,7-10), the system of R.S. Si_3N_4 surface layers on dense Si_3N_4, investigated during this contract, appears to be the only practical system investigated thus far for potential use as an energy absorbing surface layer on dense Si_3N_4 used as a high temperature structural ceramic. While the RSSN surface layers do tend to degrade the inherent bend strength of the dense Si_3N_4 substrate somewhat, and they do tend to oxidize internally in high temperature environments, these do not appear to be limiting factors in the application of the RSSN energy absorbing surface layer concept.

REFERENCES

1. Rhodes, W. H. and R. M. Cannon, Jr.: "High Temperature Compounds for Turbine Vanes", AVCO Systems Division Report, NASA CR-134531, Contract NAS3-16757 (Jan. 1974) and NASA CR-120966, Contract NAS3-14333 (Sept. 1972).

2. Brennan, J. J.: "Development of Fiber Reinforced Ceramic Matrix Composites", UTRC Report N911647-3, Contract N62269-73-C-2068 (Jan. 1974).

3. Brennan, J. J.: "Development of Fiber Reinforced Ceramic Matrix Composites", UTRC Report R911848-1, Contract N62269-74-C-0268 (Feb. 1975).

4. Platts, D. R., H. P. Kirchner and R. M. Gruver: "Strengthening Oxidation Resistant Materials for Gas Turbine Applications", Ceramic Finishing Co. Report, NASA CR-121002, Contract NAS3-15561 (Sept. 1972).

5. Gruver, R. M., D. R. Platts and H. P. Kirchner: "Strengthening Silicon Carbide by Quenching", Bull. Amer. Ceram. Soc. 53 (7) 524-527 (July 1974).

6. Kirchner, H. P.: "Strengthening of Oxidation Resistant Materials for Gas Turbine Applications", Ceramic Finishing Co. Report, NASA CR-134661, Contract NAS3-16788 (June 1974).

7. Kirchner, H. P. and J. Seretsky: "Improving Impact Resistance by Energy Absorbing Surface Layers", Ceramic Finishing Co. Report, NASA CR-134644, Contract NAS3-17765 (March 1974).

8. Palm, J. A.: "Improved Toughness of Silicon Carbide", General Electric Co., NASA CR-134921, Nov. 1975.

9. Palm, J. A.: "Improved Toughness of Silicon Carbide", NASA CR-134990, Final Report on Contract NAS3-17832 (Jan. 1976).

10. Brennan, J. J. and C.O. Hulse: "Development of Si_3N_4 and SiC of Improved Toughness", NASA CR-135306, Final Report on Contract NAS3-19731, Oct. 25, 1977.

11. Gazza, G. E., H. Knoch, and G. D. Quinn: "Hot-Pressed Si_3N_4 with Improved Thermal Stability", Bull. Am. Cer. Soc., Vol. 57, No. 11, Nov. 1978, pp 1059-1060.

12. Brennan, J. J.: "Evaluation of Tantalum Fiber Reinforced Si_3N_4", NADC-75207-30, Final Report on Contract N62269-76-C-0104, April 1, 1977.

13. Gazzara, C. P. and D. R. Messier: "Quantitative Determination of Phase Content of Silicon Nitride by X-ray Diffraction Analysis", AMMRC Report TR75-4, Feb. 1975.

14. Lindley, M. W., D. P. Elias, B. F. Jones, and K. C. Pitman: "The Influence of Hydrogen in the Nitriding Gas on the Strength, Structure and Composition of Reaction-Sintered Si_3N_4", J. Matls. Sci. 14 (1979) pp 70-85.

Table I

Spectrochemical Analysis of Norton NC-132 and
NCX-34 Si_3N_4 Impurity Content

NC-132 Si_3N_4 ρ = 3.25 gms/cc	Element	Wt % Present
	Al	0.10
	Fe	0.15
	Mg	0.35
	W	3.00
	Cr,Co,Cu, Mn,Ti,Ca,Na	<0.01 each
NCX-34 Si_3N_4 ρ = 3.35 gm/scc		
	Y	7.15*
	Fe	0.20
	Al	0.20
	Mn	0.05
	W	2.90*
	Ca	0.10
	B,Mg,Ti	<0.01 each

*Determined by atomic absorption

Table II

Grain Size of NC-132 and NCX-34 Si_3N_4

Sample	Grain Size (μ)		
	Max.	Mean	Min.
NC-132	2.4	0.80	<0.15
NCX-34	2.7	0.88	<0.15

Table III

Impurity Content of Si Powders (w/o)

Powder	Fe	Al	Mn	Mg	Pb	Cr	Ti	Ca
-325 Si (98%)	.7	.2	.3	<.01	.01	.1	.03	.1
-325 Si (99.6%)	.05	.1	<.01	<.01	.1	<.01	<.01	.05
-200 Si (98.5%)	.4	.2	.1	<.01	.02	.05	<.01	.1
-100,+200 Si (98.5%)	.3	.2	.03	<.01	.02	<.01	.02	.1

Table IV

BET (N_2) Surface Area Analysis of Si Powders

Powder Sample	Surface Area (m^2/g)
-325 Si (99.6% purity)	7.2
-325 Si (98% purity)	2.7
-200 Si (98.5% purity)	0.77

Table V

RT and 1370°C Ballistic Impact Properties of NCX-34 and NC-132
Si_3N_4 Controls Using 0.34 gm (4.4 mm) Hardened
Chrome-Steel Projectile

Sample No.	Temp (°C)	Impact Velocity		Impact Energy		Comments
		m/sec	ft/sec	joules	ft-lbs	
NCX-34-BI-1	RT	130	425	2.8	2.1	Tensile Failure
-2	"	130	425	2.8	2.1	" "
-3	"	127	415	2.7	2.0	Hertzian Failure
-4	"	127	415	2.7	2.0	Tensile Failure
-5	"	134	440	3.0	2.2	" "
	Avgs	130	425	2.8	2.1	
-6	1370	134	440	3.0	2.2	Tensile Failure
-7	"	117	385	2.3	1.7	Fracture Origin
-8	"	127	415	2.7	2.0	Uncertain
-9	"	117	385	2.3	1.7	"
-10	"	117	385	2.3	1.7	"
	Avgs	122	400	2.6	1.9	
NC-132 Averages	RT	105	345	1.9	1.4	Predominantly Hertzian Failure
"	1370	128	420	2.8	2.1	50-50 Hertzian & Tensile Failure

Table VI

RT and 1370°C Ballistic Impact Properties of NCX-34 Si_3N_4
with 1 mm Thick RSSN Layer, Nitrided 60 hrs at 1375°C

Layer	Temp. $^\circ$C	Impact Velocity		Impact Energy		Comments
		m/sec	ft/sec	joules	ft-lbs	
-325 Si	RT	191	630	6.2	4.6	Layer destroyed, no damage to substrate
"	"	230	755	9.1	6.7	Si_3N_4 substrate fractured, tensile failure
"	"	246	810	10.5	7.7	"
"	1370	169	555	4.9	3.6	Layer destroyed, no damage to substrate
"	"	191	630	6.2	4.6	Si_3N_4 substrate fractured, tensile failure
-100,+200 Si*	RT	169	555	4.9	3.6	Layer destroyed, no damage to substrate
"	"	191	630	6.2	4.6	Si_3N_4 substrate fractured, tensile failure
"	1370	152	500	3.7	2.7	Layer destroyed, no damage to substrate
"	"	169	555	4.9	3.6	Si_3N_4 substrate fractured, origin uncertain

* <5 v/o Si unreacted

Table VII

RT Ballistic Impact Properties of NC-132 and NCX-34 Si$_3$N$_4$ with 1 mm Thick RSSN Layer (-100,+200 Si), 25-30 v/o Unreacted Si Nitrided 24 hrs at 1375°C

Substrate Material	Impact Velocity		Impact Energy		Comments
	m/sec	ft/sec	joules	ft-lbs	
NC-132 Si$_3$N$_4$	191	630	6.2	4.6	Two-thirds of layer retained, no damage to substrate
"	212	695	7.6	5.6	Layer destroyed, no damage to substrate
"	230	755	9.1	6.7	"
"	246	810	10.5	7.7	Si$_3$N$_4$ substrate fractured, Hertzian failure
NCX-34 Si$_3$N$_4$	191	630	6.2	4.6	Half of layer retained, no damage to substrate
"	212	695	7.6	5.6	"
"	230	755	9.1	6.7	Layer destroyed, no damage to substrate
"	246	810	10.5	7.7	"
"	260	850	11.4	8.4	"
"	271	890	12.5	9.2	Si$_3$N$_4$ substrate fractured, tensile failure

Table VIII

RT Ballistic Impact Tests of RSSN Layers, 1 mm Thick, on NCX-34 Si_3N_4 (Nitrided to $1375^{O}C$, 8 hrs)

Layer	Impact Velocity		Impact Energy		Comments
	m/sec	ft/sec	joules	ft-lbs	
-325 Si	169	555	4.9	3.6	2/3 of layer destroyed, no damage to substrate
"	191	630	6.2	4.6	Si_3N_4 substrate fractured, tensile failure
-100,+200 Si*	260	850	11.4	8.4	layer destroyed, no damage to substrate
"	272	890	12.5	9.2	Si_3N_4 substrate fractured, tensile failure
"	282	925	13.6	10.0	"

* 60 v/o Si unreacted

Table IX

RT Ballistic Impact Properties of NC-132 and NCX-34 Si_3N_4 with 1 mm Thick RSSN Layers, Nitrided 1 hr at 1375°C, N_2

Substrate Material	Layer	Impact Velocity		Impact Energy		Comments
		m/sec	ft/sec	joules	ft-lbs	
NC-132	-200 Si*	230	755	9.1	6.7	Layer destroyed only at point of impact, no damage to substrate
"	"	260	850	11.4	8.4	Two-thirds of layer retained, no damage to substrate
"	"	282	925	13.6	10.0	Layer destroyed, no damage to substrate
"	"	300	980	15.4	11.4	Si_3N_4 substrate fractured, Hertzian failure
NCX-34	"	300	980	15.4	11.4	Half of layer destroyed, no damage to substrate
NC-132	-325 Si**	282	925	13.6	10.0	Layer destroyed, no damage to substrate
"	"	300	980	15.4	11.4	Si_3N_4 substrate fractured, Hertzian failure
NCX-34	"	300	980	15.4	11.4	Layer destroyed, no damage to substrate

* 30 v/o unreacted Si
** 20 v/o unreacted Si

45

Table X

RT Ballistic Impact Properties of NC-132 and NCX-34 Si_3N_4 with 1 mm
Thick RSSN Layers, Nitrided 1 hr at $1375^{\circ}C$ in 96% N_2/4% H_2

Substrate Material	Layer	Impact Velocity		Impact Energy		Comments
		m/sec	ft/sec	joules	ft-lbs	
NC-132	-200 Si*	260	850	11.4	8.4	Layer destroyed only at point of impact, no damage to substrate
"	"	282	925	13.6	10.0	Half of layer destroyed, no damage to substrate
"	"	300	980	15.4	11.4	Si_3N_4 substrate fractured, tensile failure
NCX-34	-200 Si*	300	980	15.4	11.4	Layer destroyed only at point of impact, no damage to substrate
"	"	315	1045	17.2	12.7	Si_3N_4 substrate fractured, Hertzian failure
NCX-34	-325 Si**	191	630	6.2	4.6	Layer destroyed, no damage to substrate
"	"	230	755	9.1	6.7	Si_3N_4 substrate fractured, Hertzian failure
"	"	260	850	11.4	8.4	Si_3N_4 substrate fractured, tensile failure

 * 21 v/o unreacted Si
** 5 v/o unreacted Si

Table XI

RT Ballistic Impact Properties of NCX-34 Si_3N_4 with 1 mm Thick RSSN
Layers, Nitrided for Various Times at $1375^{O}C$ in 96% N_2/4% H_2

Layer	Time at $1375^{O}C$ (Vol % Si)	Impact Velocity		Impact Energy		Comments
		m/sec	ft/sec	joules	ft-lbs	
-325 Si	30 min (20% Si)	343	1125	19.7	14.5	Layer destroyed, no damage to substrate
"	1 hr (5% Si)	191	630	6.2	4.6	"
'	"	230	755	9.1	6.7	Si_3N_4 substrate fractured, Hertzian failure
-200 Si	30 min (25% Si)	300	980	15.4	11.4	2/3 of layer destroyed, no damage to substrate
"	"	315	1045	17.2	12.7	Si_3N_4 substrate fractured, Hertzian failure
"	1 hr (21% Si)	300	980	15.4	11.4	Layer destroyed only at point of impact, no damage to substrate
"	"	315	1045	17.2	12.7	Si_3N_4 substrate fractured, Hertzian failure
"	1½ hrs (14% Si)	191	630	6.2	4.6	Layer destroyed, no damage to substrate
"	"	230	755	9.1	6.7	Si_3N_4 substrate fractured, tensile failure
"	2 hrs (6% Si)	191	630	6.2	4.6	Layer destroyed, no damage to substrate
"	"	230	755	9.1	6.7	Si_3N_4 substrate fractured, tensile failure

Table XII

RT and 1370°C Ballistic Impact Properties of NC-132 and NCX-34
Si_3N_4 with 1 mm Thick RSSN Layers Containing 5 vol % Residual Si
(1 hr at 1375°C, N_2/H_2)

Layer	Substrate	Temp.	Impact Velocity		Impact Energy		Comments
			m/sec	ft/sec	joules	ft-lbs	
-325 Si	NC-132	RT	169	555	4.9	3.6	Layer destroyed, no damage to substrate
"	"	RT	191	630	6.2	4.6	Si_3N_4 substrate fractured, tensile failure
"	"	1370°C	230	755	9.1	6.7	Layer destroyed, no damage to substrate
"	"	1370°C	260	850	11.4	8.4	Si_3N_4 substrate fractured, tensile failure
"	NCX-34	RT	191	630	6.2	4.6	Layer destroyed, no damage to substrate
"	"	RT	230	755	9.1	6.7	Si_3N_4 substrate fractured, Hertzian failure
"	"	1370°C	152	500	3.7	2.7	Layer virtually intact, no damage to substrate
"	"	1370°C	169	555	4.9	3.6	Si_3N_4 substrate fractured, fracture origin uncertain

Table XIII

1370°C Ballistic Impact Properties of NC-132 and NCX-34
Si_3N_4 with 1 mm Thick RSSN Layers Containing ~25 vol % Residual Si
(30 min at 1375°C, N_2/H_2)

Substrate	Layer	Impact Velocity		Impact Energy		Comments
		m/sec	ft/sec	joules	ft-lbs	
NC-132	-200 Si	300	980	15.4	11.4	Layer destroyed, no damage to substrate
"	"	315	1045	17.2	12.7	Si_3N_4 substrate fractured, Hertzian failure
NCX-34	"	260	850	11.4	8.4	Layer destroyed only at point of impact, no damage to substrate
"	"	282	925	13.6	10.0	Si_3N_4 substrate fractured, fracture origin uncertain
NC-132	-325 Si	315	1045	17.2	12.7	2/3 of layer destroyed, no damage to substrate
"	"	336	1100	19.0	14.0	Si_3N_4 substrate fractured, Hertzian failure
NCX-34	"	260	850	11.4	8.4	2/3 of layer destroyed, no damage to substrate
"	"	282	925	13.6	10.0	Si_3N_4 substrate fractured, fracture origin uncertain

Table XIV

RT Ballistic Impact Condition Needed to Fracture NC-132 Si_3N_4
with Varying Thickness RSSN Layer (25 vol % Si)

Layer	Layer Thickness	Impact Velocity		Impact Energy	
		m/sec	ft/sec	Joules	ft-lbs
-200 Si	1.0 mm	300	980	15.4	11.4
-200 Si	0.64 mm	282	925	13.6	10.0
-200 Si	0.50 mm	260	850	11.4	8.4
-200 Si	0.25 mm	212	695	7.6	5.6
None	-	105	345	1.9	1.4

Table XV

RT 4-pt Bend Tests on NC-132 and NCX-34 Si_3N_4, With and Without 1 mm Thick RSSN Surface Layers

Layer	Nitriding Treatment	Modulus of Rupture – MPa (ksi)	
		NC-132	NCX-34
None*	None	662 (96)	848 (123)
-325 Si**	Ar, 1150°C, 20 hrs	695 (101)	827 (120)
-325 Si**	Ar, 1150°C, 20 hrs + N_2, 1250°C, 24 hrs	627 (91)	690 (100)
-325 Si**	Ar, 1150°C, 20 hrs + N_2, 1250°C, 24 hrs + N_2, 1375°C, 24 hrs	327 (47.5)	414 (60) 700 (102) poor bond
-100, +200 Si**	"	405 (58.7)	462 (67)
-325 Si*	Standard Ar, 1150°C, 20 hrs + N_2, 1250°C, 24 hrs + N_2, 1375°C, 60 hrs	324 (47)	414 (60) 710 (103) poor bond
-100, +200 Si*	"	338 (49)	427 (62)
None*	"	785 (114)	725 (105)

*Average of 10 tests
**Average of 5 tests

Table XVI

RT 4-pt Bend Strength of NC-132 and NCX-34 Si_3N_4 with Well Bonded RSSN Layers Nitrided in N_2/H_2 to $1375^{\circ}C$

Substrate	Layer	Vol % Si	Modulus of Rupture*	
			MPa	ksi
NC-132	-325 Si (98%)	<5%	632	91.6
"	-325 Si (99.6%)	<5%	361	52.3
"	-100,+200 Si (98.5%)	5-10%	338	49.0
"	-325 or -200 Si (98%)	20-25%	503	73.0
NCX-34	-325 Si (98%)	<5%	640	92.8
	-325 Si (99.6%)	<5%	539	78.2 (well-bonded)
			708	103.0 (poorly-bonded)
	-100,+200 Si (98.5%)	5-10%	513	74.5
	-325 or -200 Si (98%)	20-25%	572	83.0

*Average of three tests

52

Table XVII

Weight Gain and Oxide Formation on NC-132 and NCX-34 Si_3N_4
Controls After 75 Cycles from $200 \rightarrow 1370^{\circ}C$ and $150 \rightarrow 1200^{\circ}C$

Substrate	Thermocycle	Wt Gain-mg*	Oxide Formation
NCX-34	$200 \rightarrow 1370^{\circ}C$	$8.2(0.30 \text{ mg/cm}^2)$	$Y_2Si_2O_7 + SiO_2$
NC-132	"	$23(0.85 \text{ mg/cm}^2)$	$MgSiO_3 + SiO_2 + glass$
NCX-34	$150 \rightarrow 1200^{\circ}C$	$4(0.15 \text{ mg/cm}^2)$	SiO_2 (major) + Y_2SiO_5 (minor)
NC-132	"	$6.7(0.25 \text{ mg/cm}^2)$	SiO_2 (major) + Si_2N_2O (minor) + unidentified minor phase

*average of six samples

Table XVIII

RT and 1370°C Ballistic Impact Properties of NC-132 and NCX-34 Si_3N_4 Control Samples, As-received and After 75 Thermal Cycles to 1200°C and 1370°C

Sample	Cycle	Test Temp.	Impact Velocity		Impact Energy*		Comments
			m/sec	ft/sec	joules	ft-lbs	
NC-132	None	RT	105	345	1.9	1.4	Predominantly Hertzian Failure
"	150 → 1200°C	"	117	385	2.3	1.7	"
"	200 → 1370°C	"	111	365	2.0	1.5	"
"	None	1370°C	128	420	2.8	2.1	Hertzian & Tensile Failure
"	150 → 1200°C	"	123	405	2.6	1.9	"
"	200 → 1370°C	"	120	392	2.4	1.8	"
NCX-34	None	RT	130	425	2.8	2.1	Predominantly Tensile Failure
"	150 → 1200°C	"	140	458	3.3	2.4	"
"	200 → 1370°C	"	135	444	3.1	2.3	"
"	None	1370°C	122	400	2.6	1.9	Fracture Origins Uncertain
"	150 → 1200°C	"	133	438	3.0	2.2	"
"	200 → 1370°C	"	115	378	2.2	1.6	"

*average of 5 tests

Table XIX

Ballistic Impact Energy Necessary to Fracture NC-132 and NCX-34
Si_3N_4 Substrates with 1 mm Thick RSSN Layers (20-25% Si),
As-Fabricated and After 75 Cycles from 150°C→1200°C and 200°C→1370°C

Substrate	Layer	Treatment	Test Temp.	Impact Velocity		Impact Energy		Comments
				m/sec	ft/sec	joules	ft-lbs	
NCX-34	-200 Si	none	RT	315	1045	17.2	12.7	Hertzian failure
"	"	cycled to 1200°C	"	336	1100	19.0	14.0	"
"	"	cycled to 1370°C	"	336	1100	19.0	14.0	Tensile failure
"	"	none	1370°C	282	925	13.6	10.0	Indeterminate failure
"	"	cycled to 1200°C	"	300	980	15.4	11.4	Hertzian failure
"	"	cycled to 1370°C	"	315	1045	17.2	12.7	Tensile failure
NC-132	-325	none	RT	300	980	15.4	11.4	Hertzian failure
"	"	cycled to 1200°C	"	300	980	15.4	11.4	"
"	"	cycled to 1370°C	"	315	1045	17.2	12.7	"
"	-200	none	"	300	980	15.4	11.4	Tensile failure
"	"	cycled to 1200°C	"	300	980	15.4	11.4	Hertzian failure
"	"	cycled to 1370°C	"	>336	1100	19.0	14.0	No fracture
"	"	none	1370°C	315	1045	17.2	12.7	Hertzian failure
"	"	cycled to 1200°C	"	336	1100	19.0	14.0	"
"	"	cycled to 1370°C	"	336	1100	19.0	14.0	"

Table XX

Weight Gain and Oxide Formation for NC-132 Si_3N_4
with -200 RSSN Surface Layers after 75 Cycles from
$200^\circ C \rightarrow 1370^\circ C$, Both With and Without CVD SiC Overlayers

Substrate	Layer	Overlayer	Thermocycle	Wt Gain (mg)	Oxide Formation
NC-132	none	none	$200 \rightarrow 1370^\circ C$	23	$MgSiO_3$ + SiO_2 + glass
"	-200 Si	none	"	153	α-cristobalite (SiO_2)
"	"	CVD SiC	"	52	"

56

Table XXI

Ballistic Impact Energy Necessary to Fracture NC-132 Si_3N_4 With 1 mm Thick RSSN Layers (20-25 vol % Si), As-Fabricated and After 75 Cycles from 200→1370°C Both With and Without CVD SiC Overlayers

Substrate	Layer	Overlayer	Treatment	Test Temp	Impact Velocity		Impact Energy	
					m/sec	ft/sec	joules	ft-lbs
NC-132	-200 Si	none	none	RT	300	980	15.4	11.4
"	"	CVD SiC	none	"	300	980	15.4	11.4
"	"	none	cycled to 1370°C	"	336	1100	19.0	14.0
"	"	CVD SiC	"	"	315	1045	17.2	12.7

Note: Values for 1370°C test results are comparable

Table XXII

Ballistic Impact Properties of Thermally Cycled* RSSN/HPSN Combinations

Layer	Thermal Cycle	Impact Energy for Substrate Fracture (joules)			
		NC-132 Si$_3$N$_4$		NCX-34 Si$_3$N$_4$	
		RT	1370°C	RT	1370°C
None	None	1.9	2.8	2.8	2.6
"	75 cycles, 150→1200°C	2.3	2.6	3.3	3.0
"	75 cycles, 200→1370°C	2.0	2.4	3.1	2.2
-200 Si(20-25 v/o Si)	None	15.4	–	17.2	13.6
"	75 cycles, 150→1200°C	15.4	–	19.0	15.4
"	75 cycles, 200→1370°C	19.0	–	19.0	17.2
-200 Si + CVD SiC	None	15.4	–	–	–
"	75 cycles, 200→1370°C	17.2	–	–	–
				–	
-325 Si(20-25 v/o Si)	None	15.4	17.2	–	–
"	75 cycles, 150→1200°C	15.4	19.0	–	–
"	75 cycles, 200→1370°C	17.2	19.0	–	–

*Cycle = 15 min heatup + 40 min hold + 10 min cold air blast cool

Table XXIII

Mach 0.8, 5 hr, Hot Gas Erosion Testing of NC-132 and NCX-34 Si_3N_4 Controls and RSSN Surface Layers

Substrate	Layer	Test Temp.	Surface Recession	Wt. Change	Surface X-ray Analysis
NCX-34	None	1200°C	Not Detectable	0	$\beta-Si_3N_4$
NC-132	None	"	"	0	"
NCX-34	-200 Si	"	"	+21.2 mg	$\alpha-Si_3N_4$, $\beta-Si_3N_4$, Si, SiO_2
NCX-34	-325 Si	"	"	+17.1 mg	"
NCX-34	-200 Si + CVD Si_3N_4	"	"	+22.0 mg	$\alpha-Si_3N_4$
NC-132	-200 Si + CVD SiC	"	"	+ 6.0 mg	$\beta-SiC$
NC-132	None	1370°C	0.1 mils (2.5µ)	+0.1 mg	$\beta-Si_3N_4 + SiO_2$ (minor)
NCX-34	None	"	1.0 mils (25µ)	-3.5 mg	"
NC-132	-325 Si	"	0.3 mils (8µ)	+12.4 mg	$\alpha-Si_3N_4$, $\beta-Si_3N_4$, Si, SiO_2
NC-132	-200 Si	"	0.3 mils (8µ)	+12.2 mg	"
NC-132	-325 Si + CVD Si_3N_4	"	Not Detectable	+33 mg	$\alpha-Si_3N_4 + SiO_2$ (Minor)
NCX-34	-200 Si + CVD SiC	"	"	+2.5 mg	$\beta-SiC + SiO_2$ (minor)

59

FIG. 1

MICROSTRUCTURE OF NC—132 (a) AND NCX—34 (b) HOT—PRESSED Si$_3$N$_4$ (TEM REPLICA)

a)

1μ

b)

1μ

60

79—01—63—1

NCX–34 Si$_3$N$_4$ SAMPLE FROM BILLET F 338355 SHOWING MICROCRACKS
ENHANCED BY ZYGLO PENETRANT

1 cm

FIG. 3
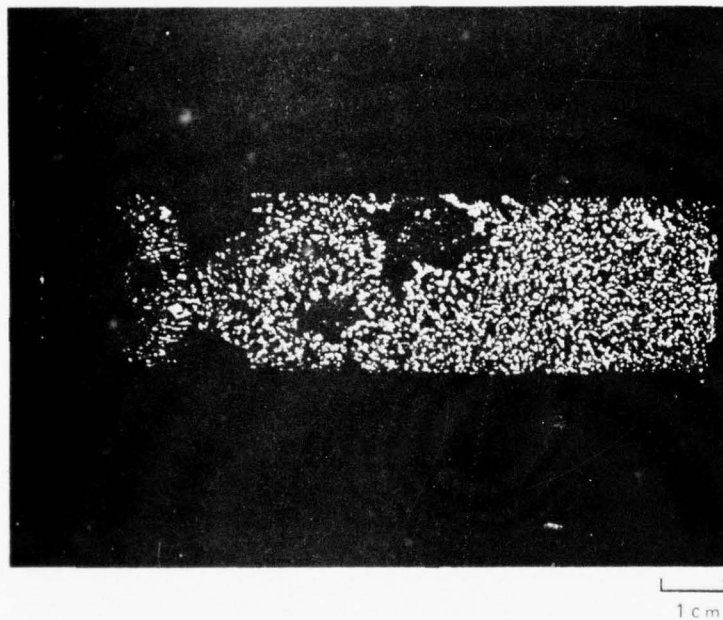
NCX—34 Si$_3$N$_4$ OXIDATION STUDY

100 HR 930°C

BEFORE

AFTER

1 CM

62

78—10—259—4

FIG. 17

FIG. 4

NCX–34 Si$_3$N$_4$ (BILLET F338355) AGED IN AIR AT 730°C FOR 48 HRS

←— TOP VIEW

←— SIDE VIEW

⊢————⊣
1.2 cm

79–01–63–2
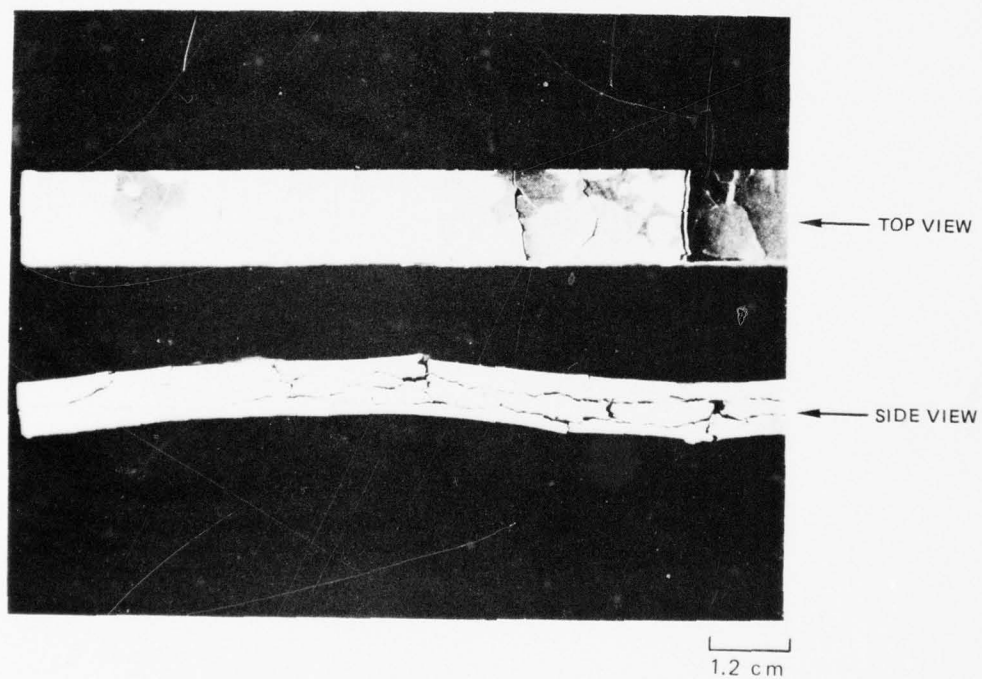
FIG. 5

STEPS IN FABRICATION OF HPSN/RSSN BALLISTIC IMPACT SAMPLES

C) AFTER GRINDING RSSN LAYER TO 1 MM THICKNESS

B) As–NITRIDED

A) DRIED S POWDER SLURRY
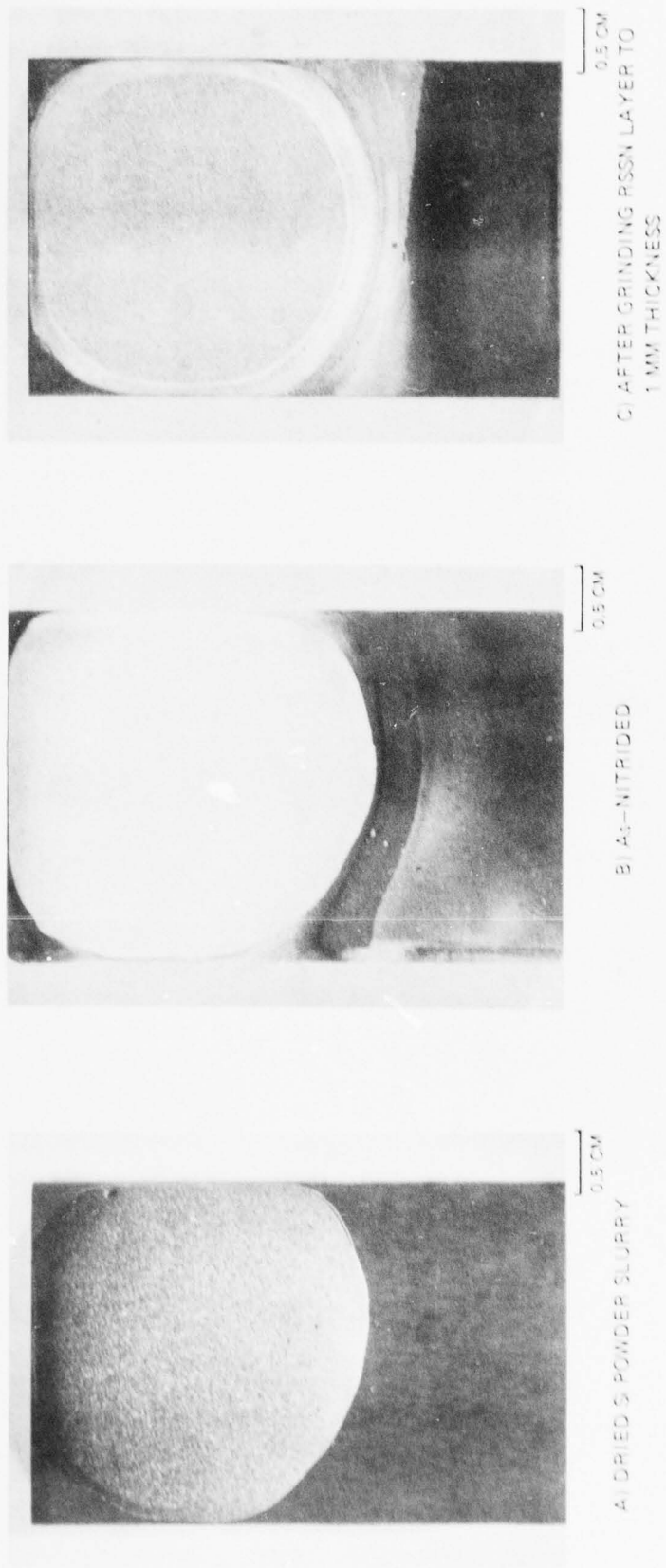
INTERFACE BETWEEN −100, +200 RSSN LAYER AND NCX−34 Si$_3$N$_4$,
NITRIDED TO 1375°C, 60 HRS, N$_2$

←− −100, +200 RSSN LAYER
   (<5 V/O UNREACTED Si)

←−−−−−− NCX−34 Si$_3$N$_4$

50μ
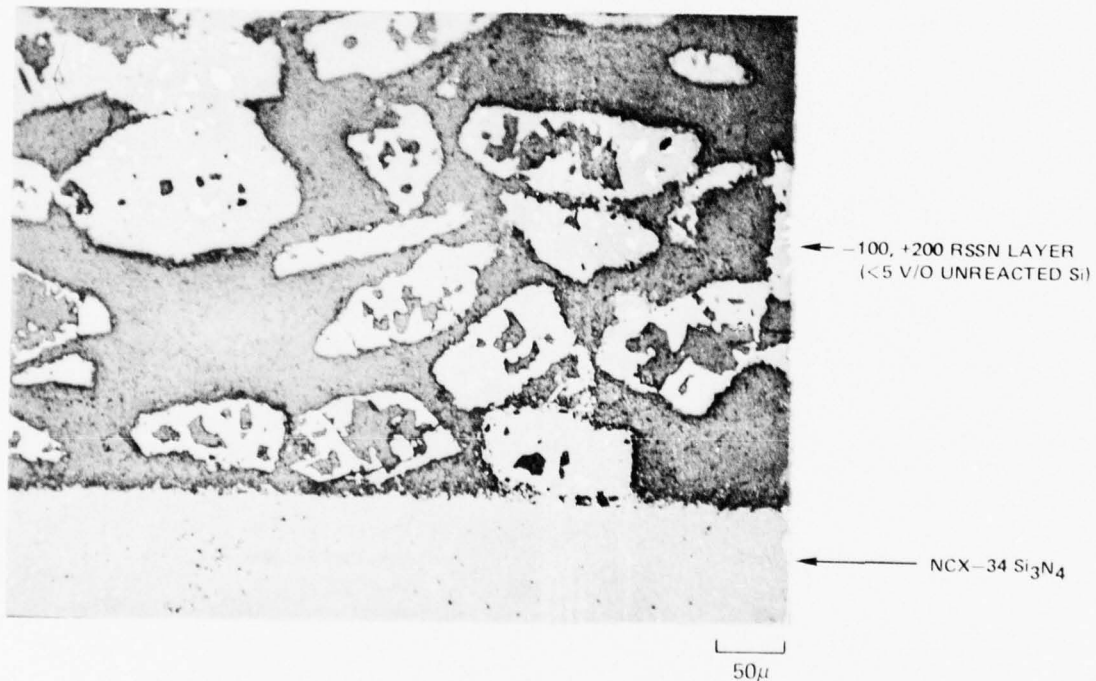
65

RSSN LAYER (−100, +200 Si) NITRIDED TO 1375ºC, 24 HRS, N$_2$
(25−30 V/O UNREACTED Si)

50μ

FIG. 8

RSSN LAYER (−100, +200 Si) NITRIDED TO 1375°C, 8 HRS, N_2
(60 V/O UNREACTED Si)

50μ

RSSN LAYER (−325 Si) NITRIDED TO 1375ºC, 8 HRS, N$_2$
(Si COMPLETELY NITRIDED)

50μ

68

FIG. 10

RSSN LAYER (−100, +200 Si) NITRIDED TO 1300°C, 8 HRS, N_2
(10 V/O OF Si CONVERTED TO Si_3N_4)

50μ

69

BALLISTIC IMPACT SAMPLE OF NC–132 Si_3N_4 WITH –200 RSSN
LAYER AFTER 9.1 JOULE IMPACT

0.5cm

RSSN LAYER (−200 Si) NITRIDED TO 1375ºC, 1 HR, 96% N_2/4% H_2
(21 V/O UNREACTED Si)

50µ

71

FIG. 13
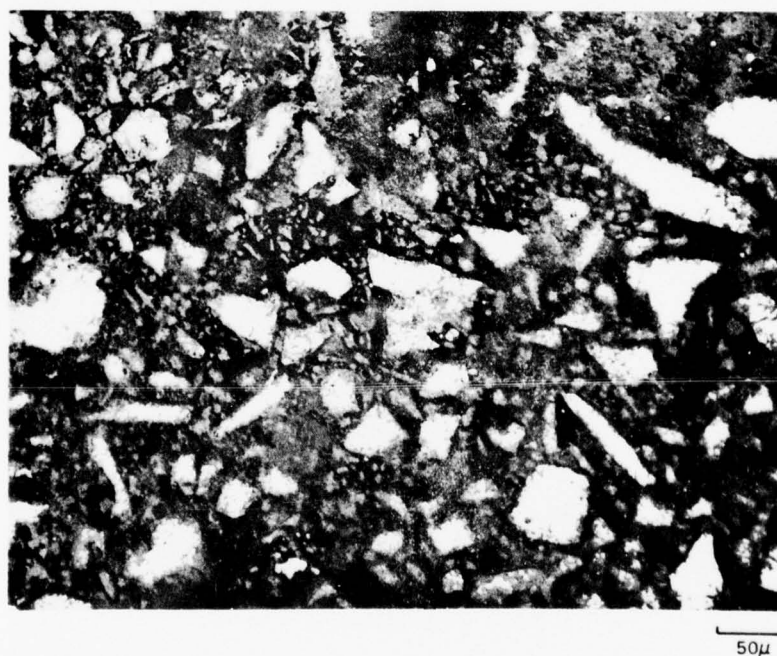
RSSN LAYER (–325 Si) NITRIDED TO 1375°C, 1 HR, 96% N_2/4% H_2
(5 V/O UNREACTED Si)

50μ
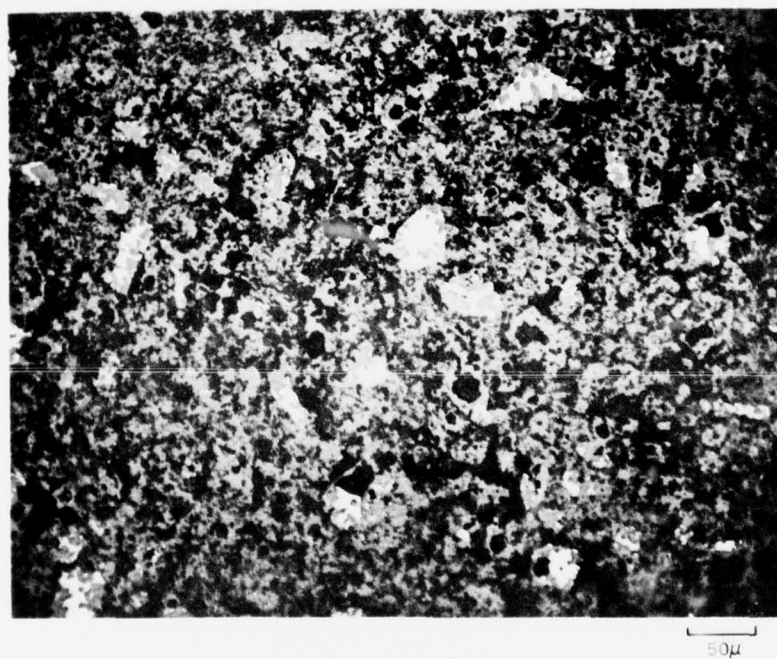
7.2

BALLISTIC IMPACT SAMPLE OF NCX–34 Si_3N_4 WITH –200 RSSN
LAYER (21 V/O Si) AFTER 15.4 JOULE IMPACT

0.4cm

73

79–04–80–7

FIG. 15

BALLISTIC IMPACT SAMPLE OF NCX–34 Si_3N_4 WITH –200 RSSN
LAYER (21 V/O Si) AFTER 17.2 JOULE IMPACT

0.4cm

74

BALLISTIC IMPACT SPECIMEN OF NCX—34 Si_3N_4 WITH —325 RSSN LAYER (5 V/O Si)
IMPACTED AT 1370°C, 169 M/SEC (4.9 JOULES)

0.5cm

FIG. 17
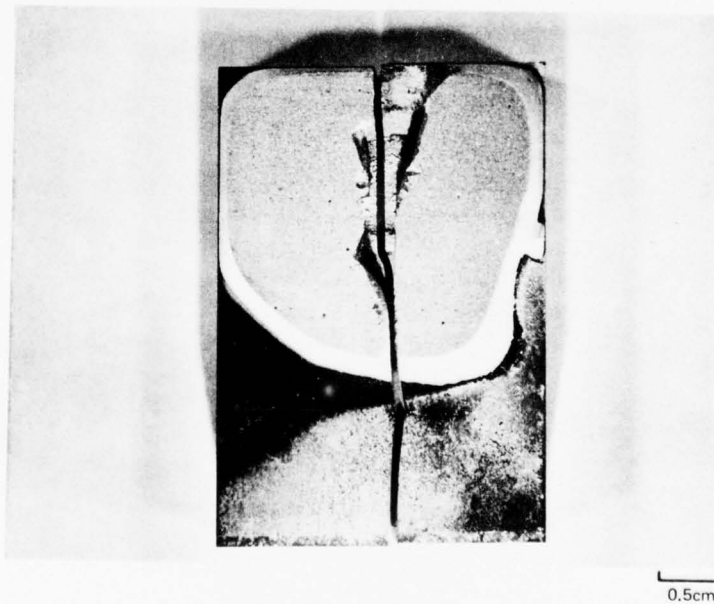
FRACTURE SURFACE OF BALLISTIC IMPACT SPECIMEN SHOWN IN FIG. 16

FRACTURE ORIGIN

POINT OF IMPACT

0.5cm

FIG. 18
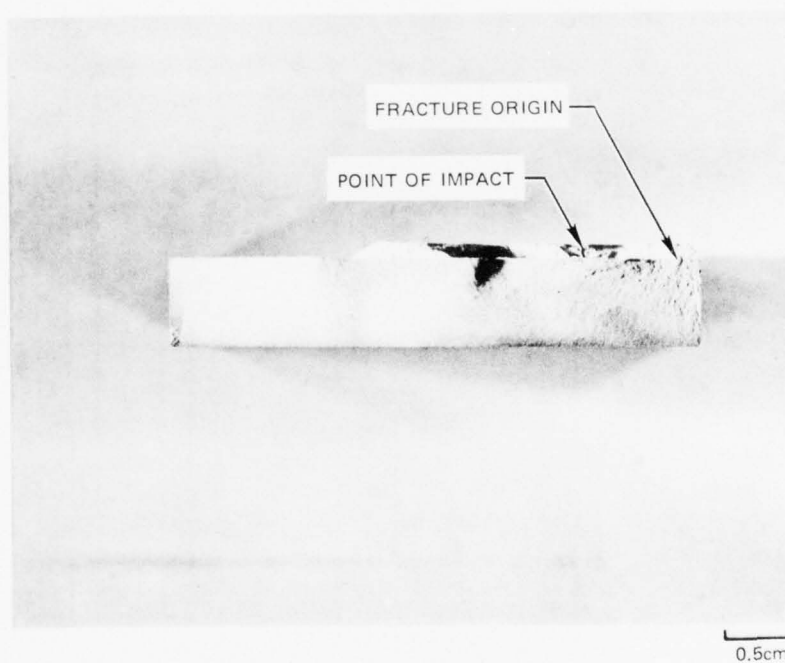
Ballistic Impact Properties of NC·132 Si₃N₄ with RSSN Energy Absorbing Surface Layers

FIG. 19
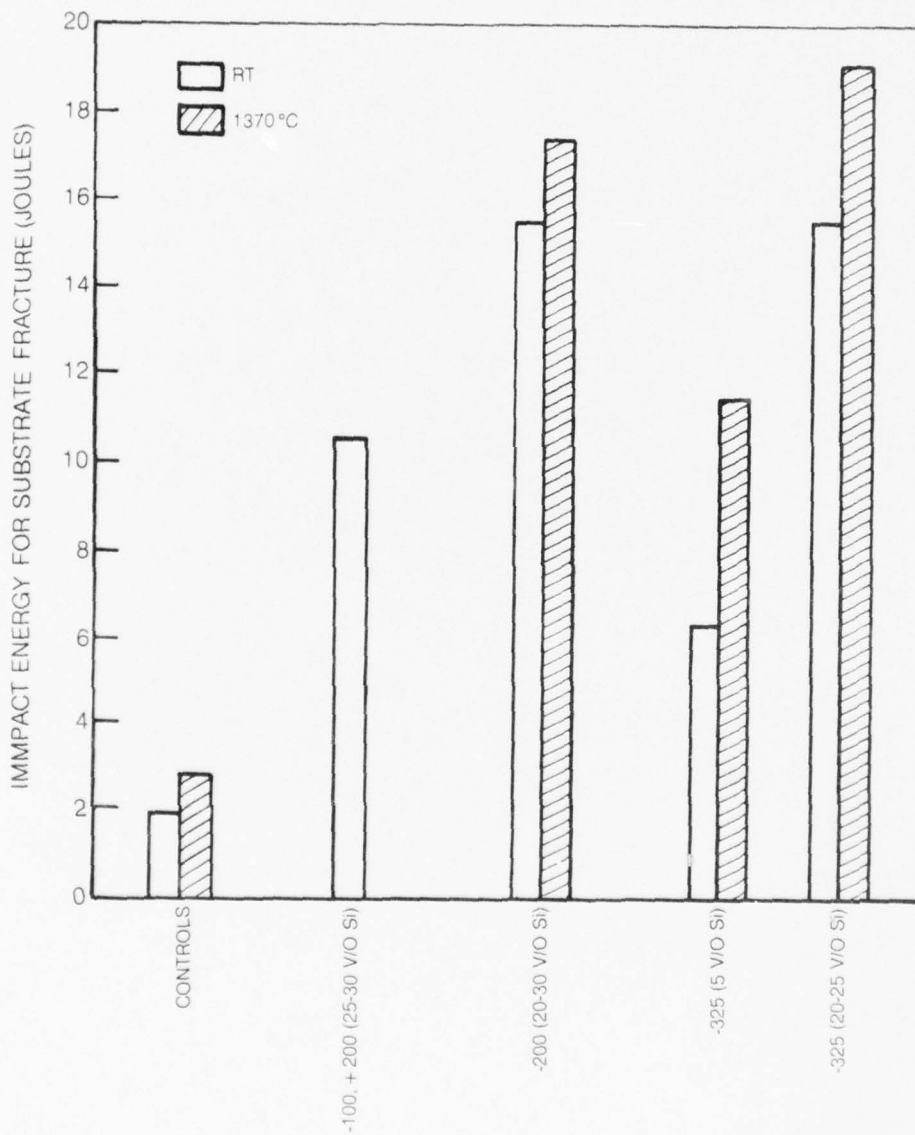
Ballistic Impact of Properties of NCX-34 Si₃N₄ with RSSN Energy Absorbing Surface Layers

FIG. 20
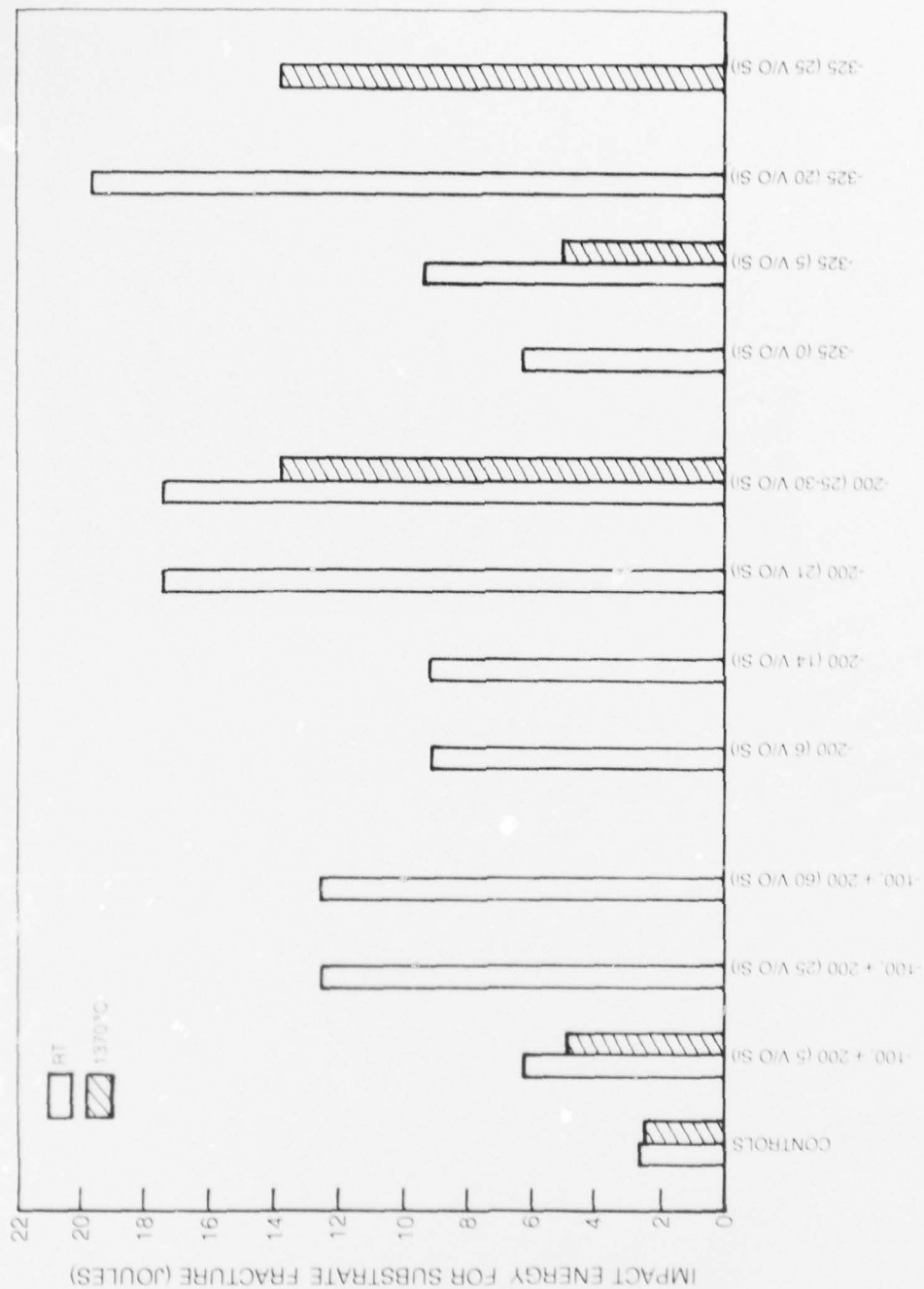
IMPACT SURFACE OF A STEEL SPHERE AFTER 130 M/SEC (2.8 JOULES) IMPACT
WITH NCX—34 Si_3N_4 CONTROL

a)   400μ

b)   200μ

79

FIG. 21
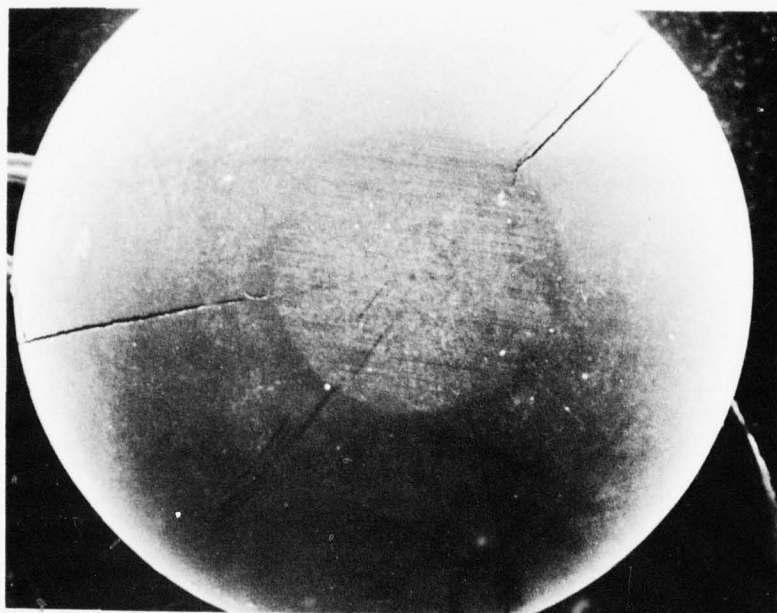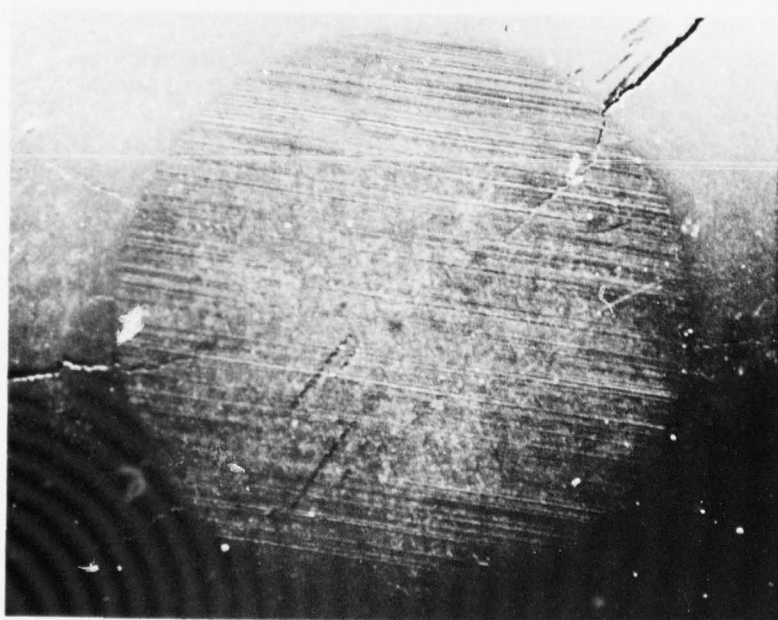
IMPACT SURFACE OF A STEEL SPHERE AFTER 230 M/SEC (9.1 JOULES)
IMPACT WITH A —200 RSSN LAYER (6 V/O Si) ON NCX—34 Si$_3$N$_4$

a)

400μ

b)

80

200μ

FIG. 22
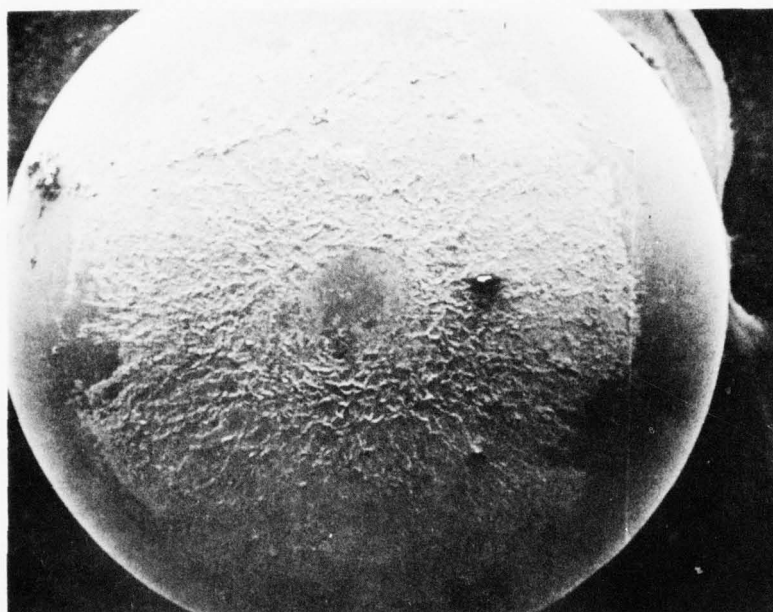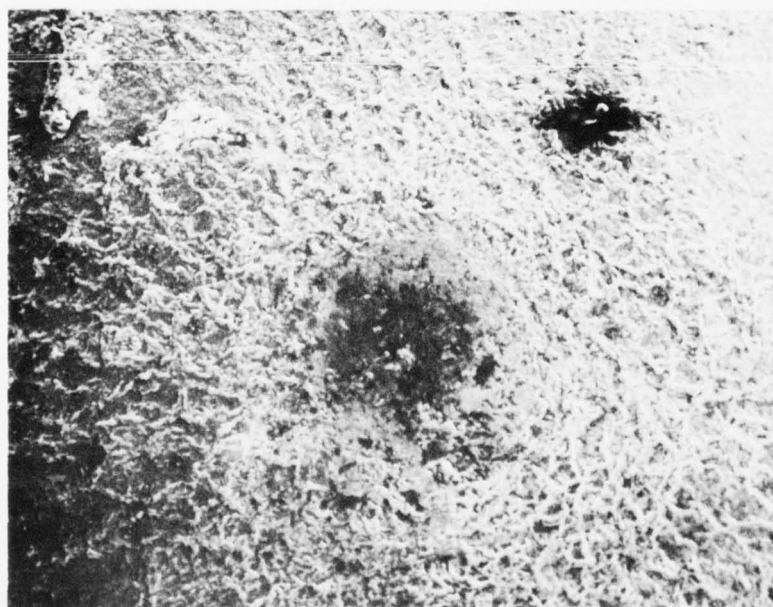
IMPACT SURFACE OF A STEEL SPHERE AFTER 260 M/SEC (11.4 JOULES) IMPACT
WITH A–200 RSSN LAYER (21 V/O Si) ON NCX–34 Si_3N_4

a)

400μ

b)

200μ

81

79-04-80-13
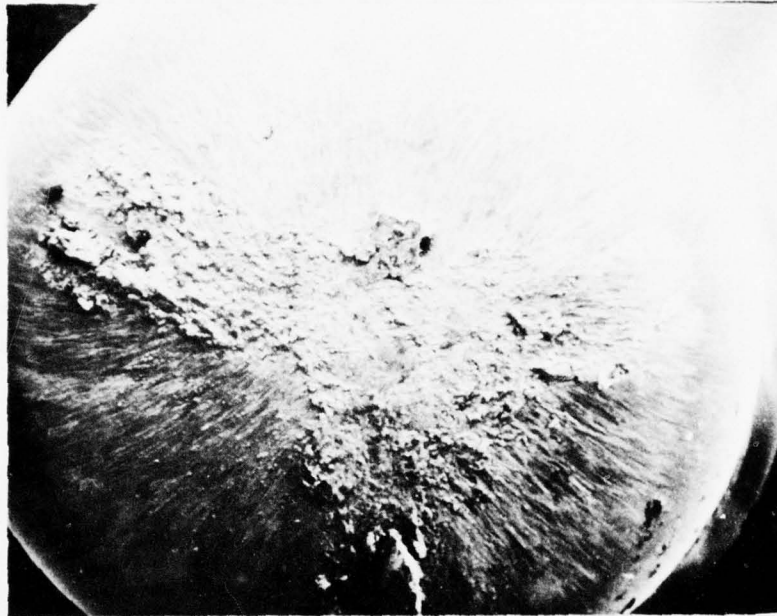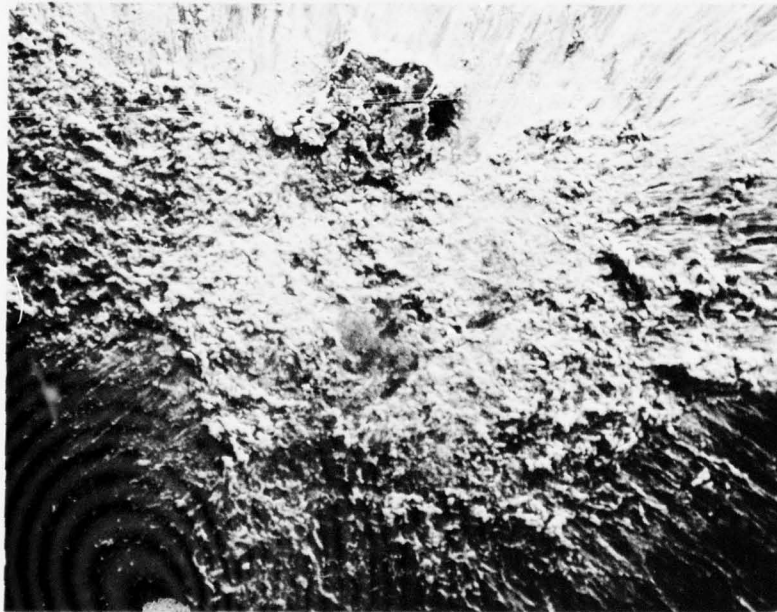
POINT OF IMPACT THROUGH A–200 RSSN LAYER DOWN TO THE HPSN SUBSTRATE
FOR A STEEL SPHERE TRAVELING AT 300M/SEC

400μ

82

FIG. 24

FRACTURE SURFACE OF NC–132 Si₃N₄ WITH –325 Si LAYER (NITRIDED AT
MAXIMUM TEMP. OF 1250°C FOR 24 HRS.)

A)

800μ

B)

100μ

C)

20μ

78–10–170–4

FIG. 25
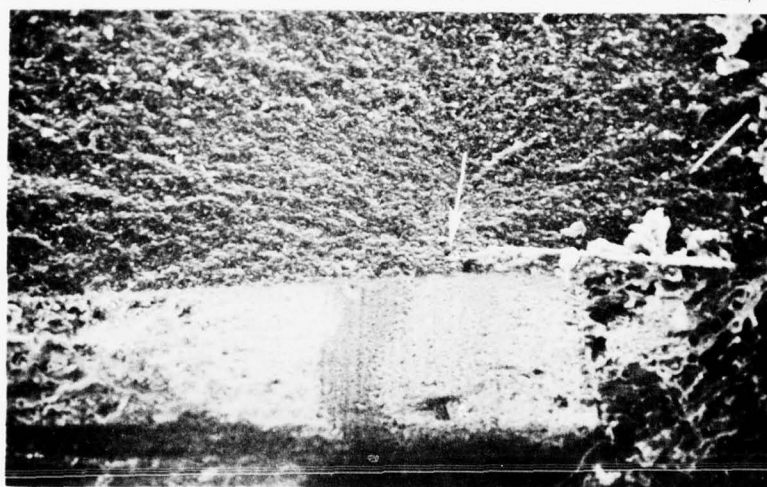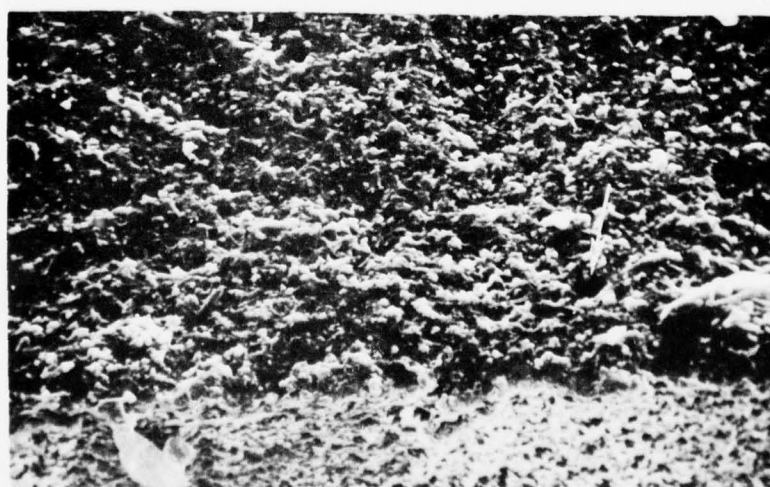
FRACTURE SURFACE OF NC–132 Si$_3$N$_4$ WITH –325 Si LAYER (NITRIDED AT
MAXIMUM TEMP. OF 1375°C FOR 24 HRS.)

A) 800μ

B) 100μ

C) 20μ

FIG. 26
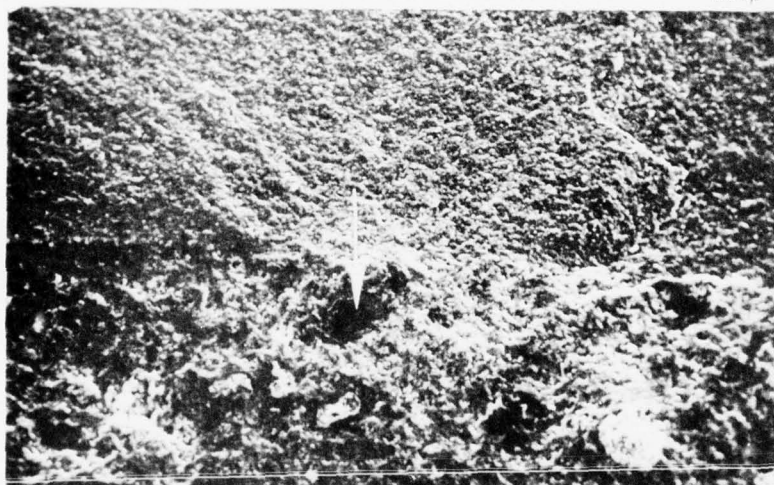
FRACTURE SURFACE OF POORLY BONDED RSSN LAYER (−325 Si, 98%) ON NCX−34 Si$_3$N$_4$, NITRIDED TO 1375ºC, 60 HRS, N$_2$

OVERALL VIEW

$\overline{800\mu}$

ORIGIN AREA

$\overline{100\mu}$

85

79−01−63−8

FRACTURE SURFACE OF STRONGLY BONDED RSSN LAYER (−100, +200 Si)
ON NCX−34 Si_3N_4, NITRIDED TO 1375°C, 60 HRS, N_2

OVERALL VIEW 800μ

ORIGIN AREA 100μ

FIG. 28
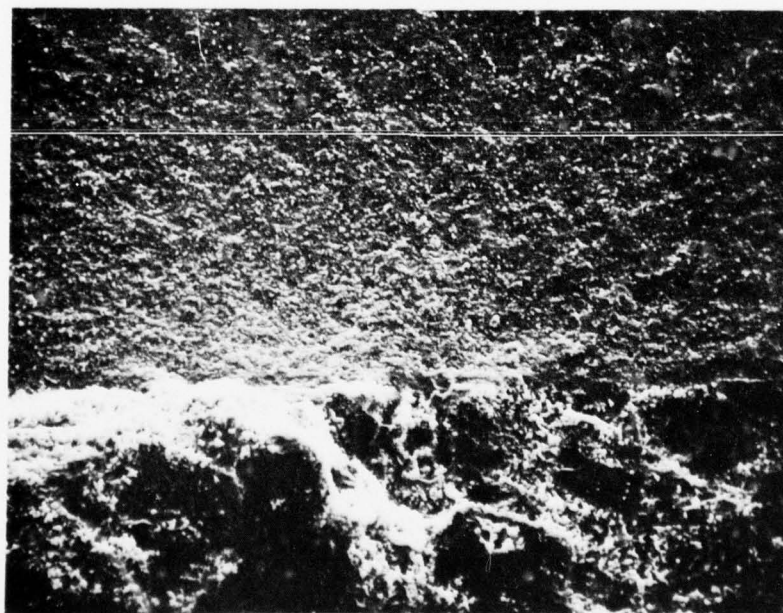
FRACTURE ORIGIN OF NCX–34 Si_3N_4 WITH LOOSE –100, +200 Si PARTICLES

ON THE SURFACE, NITRIDED TO 1375°C, 60 HRS, N_2

100μ

87

20μ

FIG. 29

FRACTURE SURFACE OF −325 Si (98%) RSSN LAYER ON NC−132 Si_3N_4,
NITRIDED IN 96% N_2/ 4% H_2 TO 1375°C, 60 HRS
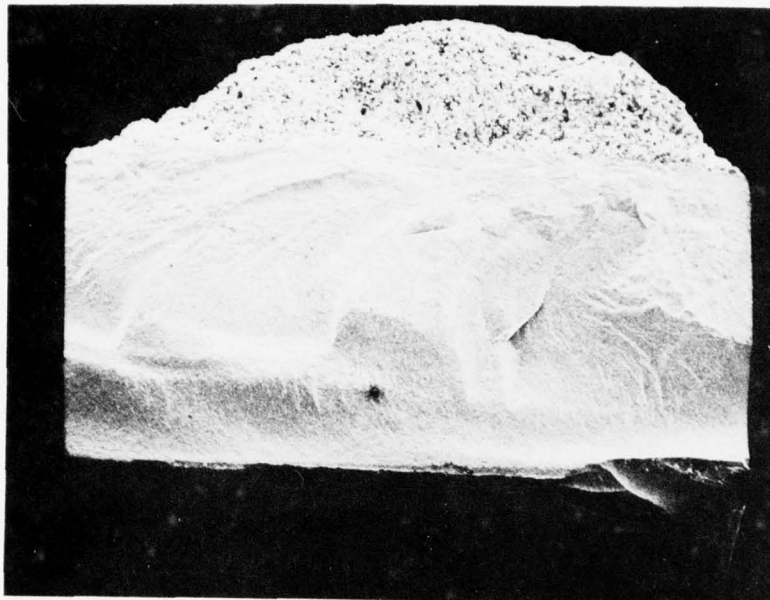
OVERALL VIEW

625μ

ORIGIN AREA

100μ

88

FRACTURE SURFACE OF −325 Si (98%) RSSN LAYER ON NCX−34 Si_3N_4,
NITRIDED IN 96% N_2/4% H_2 TO 1375°C, 60 HRS

625μ

OVERALL VIEW

100μ

ORIGIN AREA

89

79−01−72−2
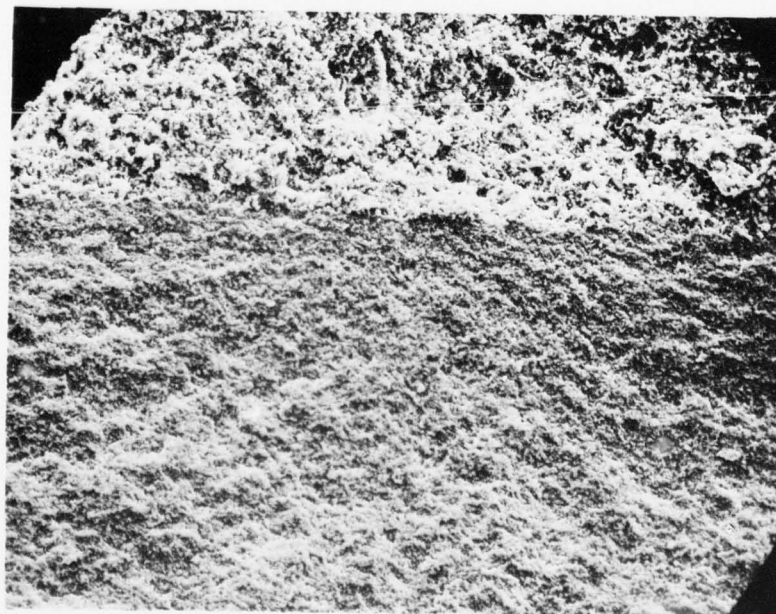
FRACTURE SURFACE OF −325 Si (98%) RSSN LAYER ON
NC−132 Si₃N₄, NITRIDED IN N₂ TO 1375°C, 60 HRS
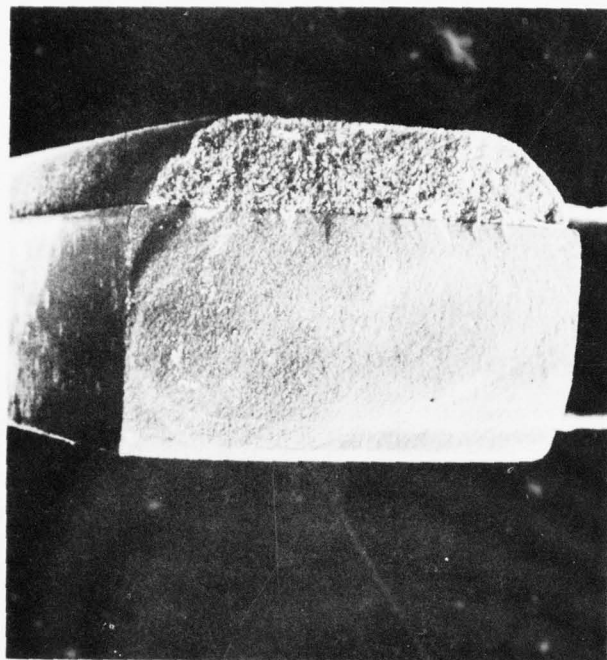
OVERALL VIEW

800μ
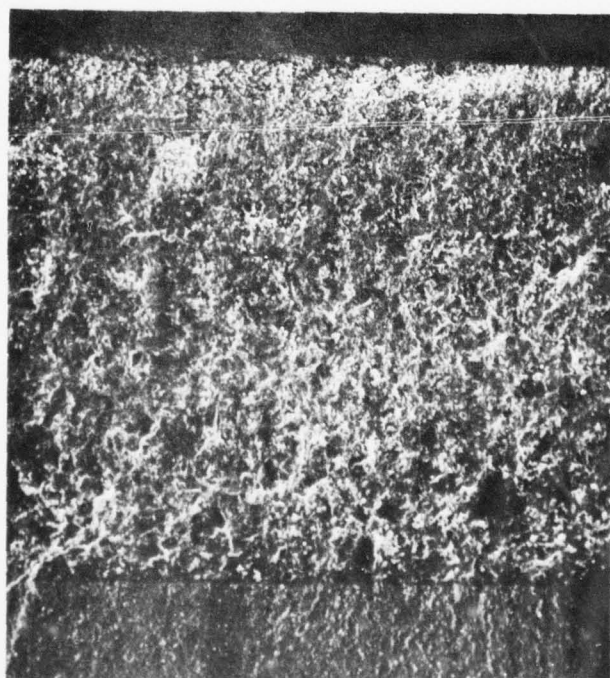
ORIGIN AREA

140μ

90

Effect of RSSN Layer on R.T. 4-Pt. Bend Strength of NC-132 Si₃N₄

HEAT TREATMENTS {
A: Ar, 1150C, 20 hrs
B: N₂, 1250C, 24 hrs
C: N₂, 1375C, 24 hrs
D: N₂, 1375C, 60 hrs
E: 96N₂/4H₂, 1250C, 24 hrs
F: 96N₂/4H₂, 1375C, 60 hrs
G: 96N₂/4H₂, 1375C, 1/2 hr
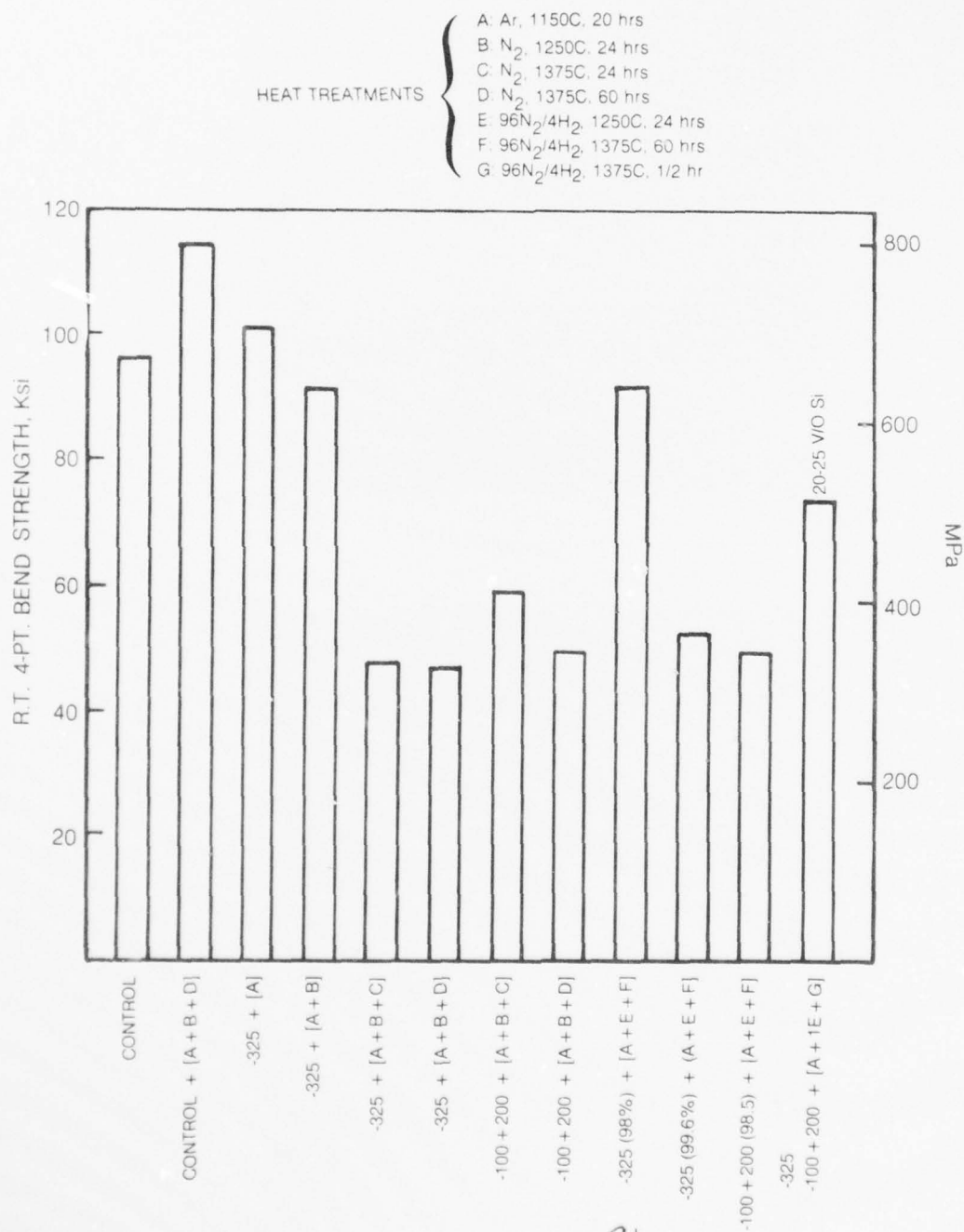
AD-A077 026   UNITED TECHNOLOGIES RESEARCH CENTER EAST HARTFORD CONN   F/G 7/2
                  DEVELOPMENT OF SILICON NITRIDE OF IMPROVED TOUGHNESS.(U)
                  OCT 79   J J BRENNAN   NAS3-21375
UNCLASSIFIED   UTRC/R79-914364-12   NASA-CR-159676   NL

2 OF 2
AD
A077026
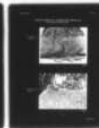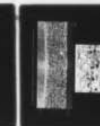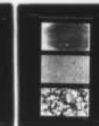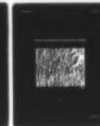
Effect of RSSN Layer on R.T. 4-Pt. Bend Strength of NCX-34 Si_3N_4

HEAT TREATMENTS {
A: Ar, 1150C, 20 hrs
B: N_2, 1250C, 24 hrs
C: N_2, 1375C, 24 hrs
D: N_2, 1375C, 60 hrs
E: $96N_2/4H_2$, 1250C, 24 hrs
F: $96N_2/4H_2$, 1375C, 60 hrs
G: $96N_2/4H_2$, 1375C, 1/2 hr
}

92

79–09–135–4

FIG. 34
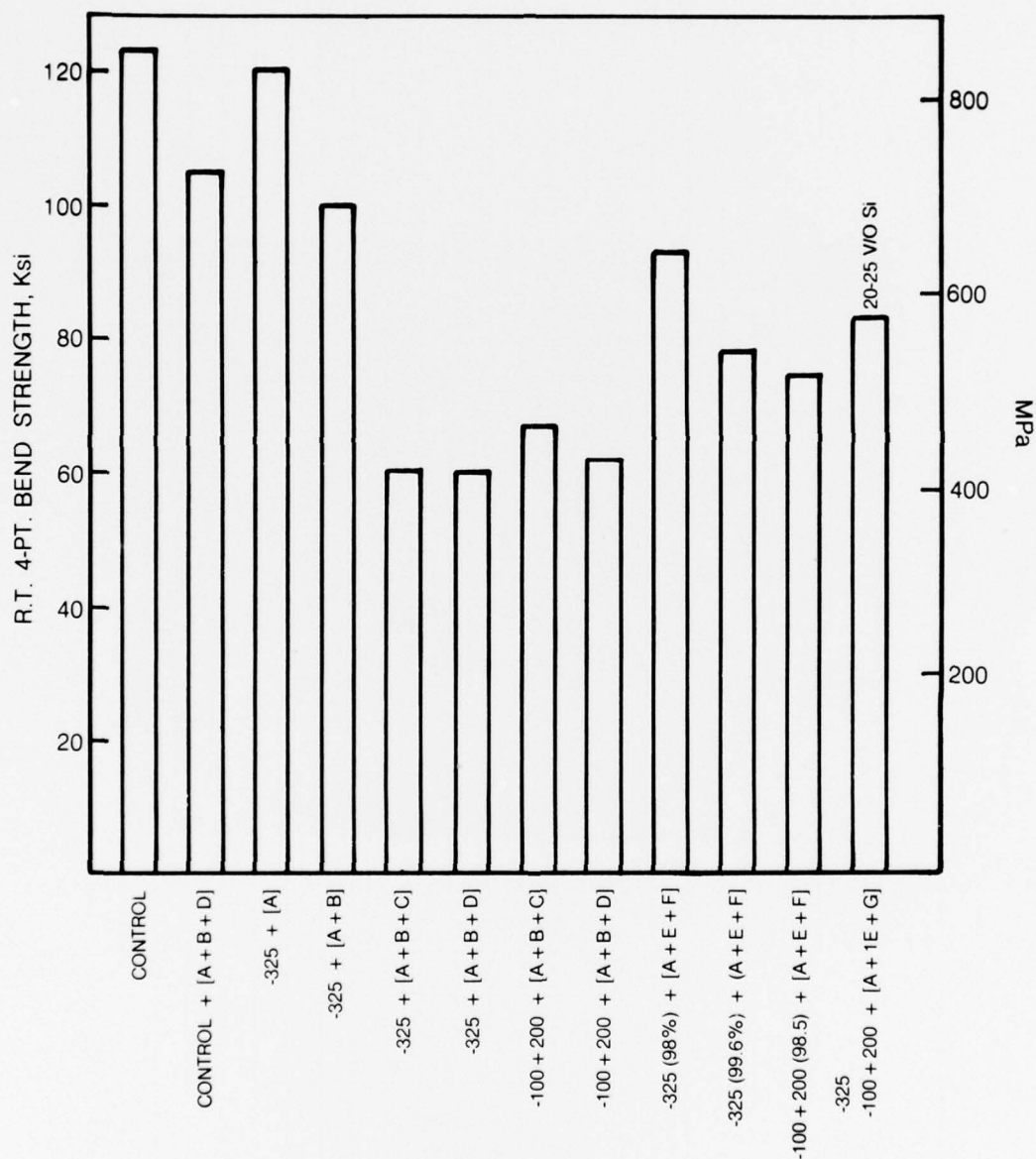
NCX–34 Si$_3$N$_4$ (LEFT) AND NC–132 Si$_3$N$_4$ (RIGHT) SAMPLES EXPOSED FOR
75 CYCLES FROM 200°C TO 1370°C,

0.5cm

73
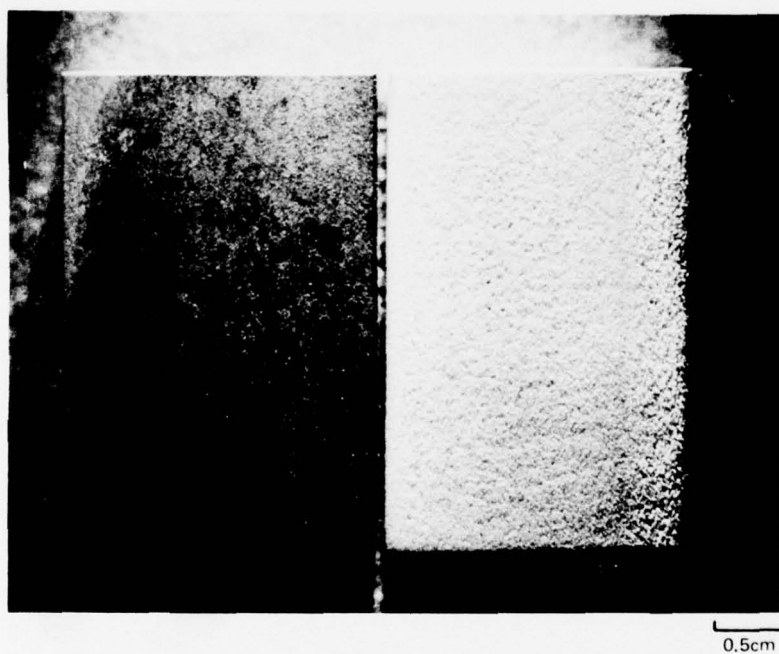
RSSN LAYER (−200 Si) ON NC−132 Si$_3$N$_4$ AFTER 75 CYCLES TO 1370ºC

A)

$\overline{}\ \underline{}$
50μ
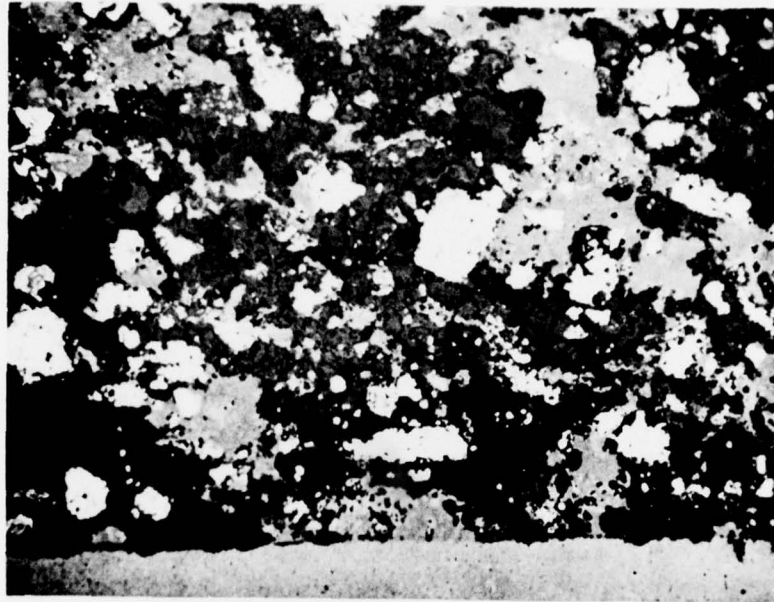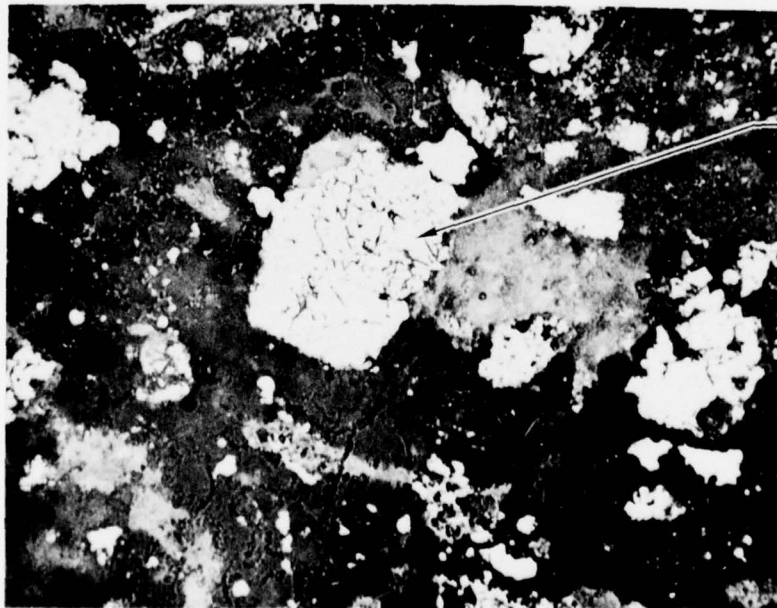
S GRAIN BOUNDARY
OXIDATION

B)

$\overline{}\ \underline{}$
20μ

94

79−06−156−2

THICK (0.15MM) CVD Si C ON – 200 RSSN/HPSN BALLISTIC IMPACT SAMPLE

50μ

95

THERMALLY CYCLED (21 CYCLES TO 1370°C) SAMPLE OF $-$200 RSSN ON NC$-$132 Si$_3$N$_4$
WITH THICK (0.15 MM) CVD SiC OVERLAYER

0.5 CM

96

FIG. 38
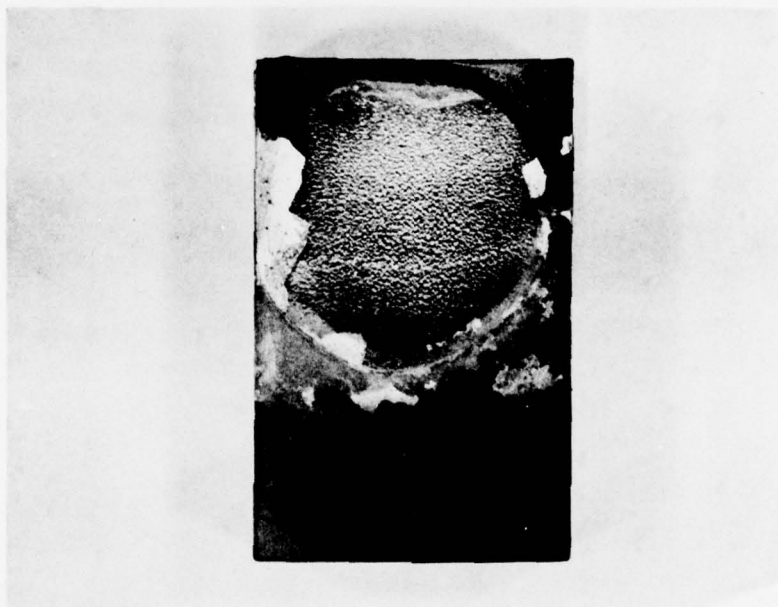
THIN (25μ), FINE GRAINED CVD Si C OVERLAYER ON –200 RSSN

20μ

97

FIG. 39
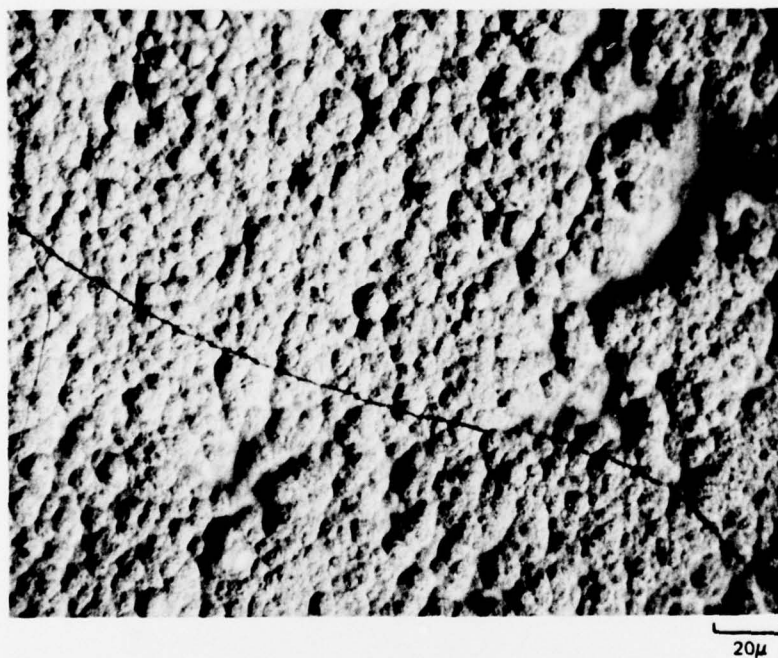
OXIDIZED SURFACE OF CVD SiC OVERLAYER AFTER 75 CYCLES TO 1370ºC.

10μ

98

79-06-156-10

FIG. 40

SEM OF NC-132 Si_3N_4 EROSION SAMPLE TESTED AT 1370°C, 5 HRS.

A)

250μ

B)

100μ

C)

99

5μ

79-06-156-3
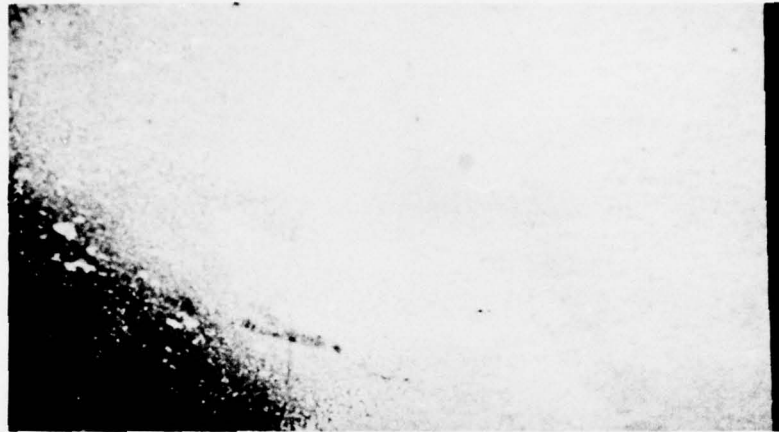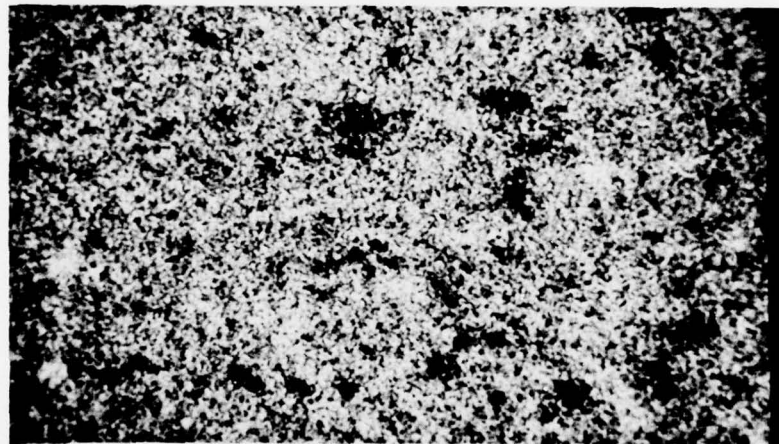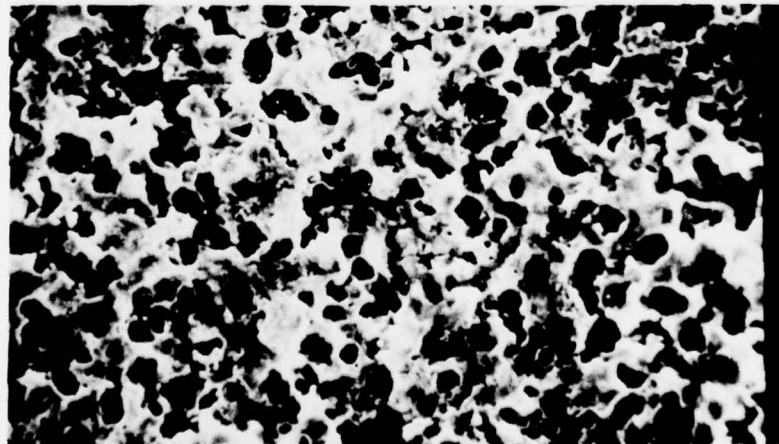
SEM OF NCX–34 Si$_3$N$_4$ EROSION SAMPLE TESTED AT 1370ºC, 5 HRS.

A)

250μ

B)

100μ

C)

5μ

FIG. 42
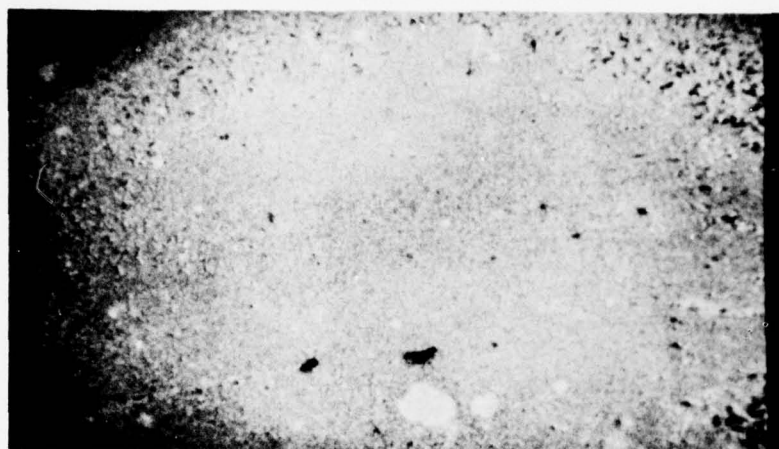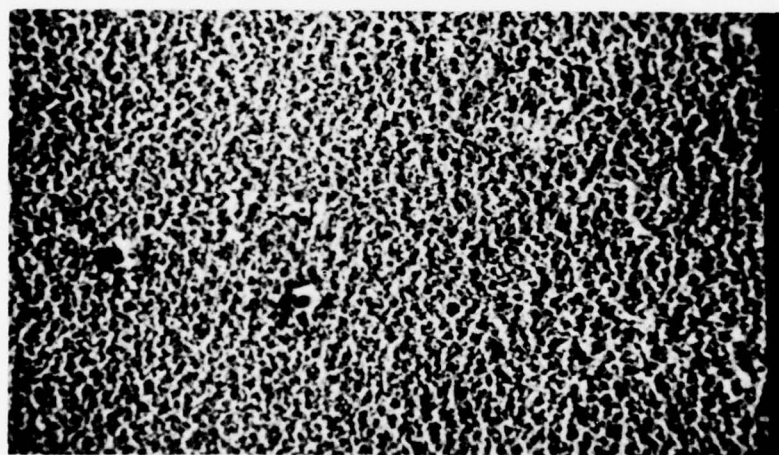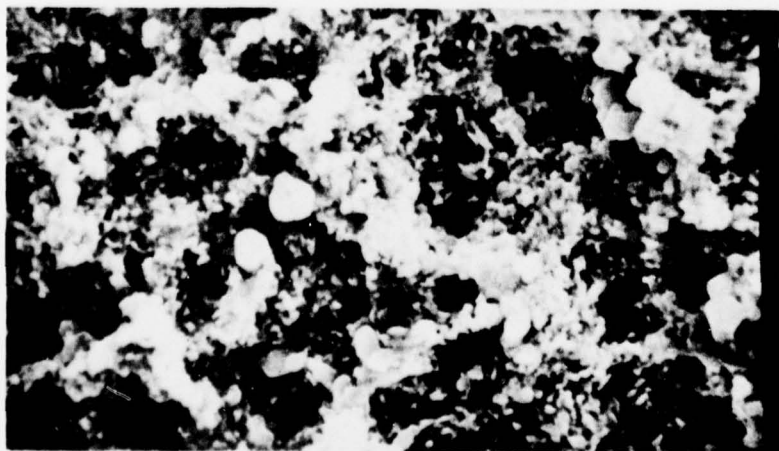
NC-132 Si₃N₄ WITH -200 RSSN LAYER (25% Si) AFTER 1370°C, 5 HR. MACH 0.8 EROSION TEST

200μ

50μ

MOUNTING MATERIAL

RSSN LAYER

NC-132 SUBSTRATE

FIG. 43

HOT GAS EROSION TEST SAMPLES AFTER 5 HRS. AT 1370ºC
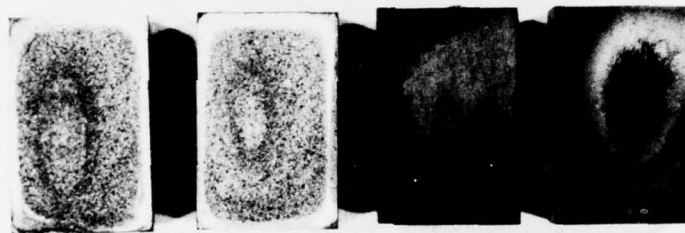
| −200 RSSN | −325 RSSN | NC−132 | NCX−34 |

0.5 CM

102

SEM OF –200 RSSN EROSION SAMPLES TESTED AT (A) 1200ºC, 5 HRS.,
AND (B) 1370ºC, 5 HRS.

A)

10μ

B)

113

10μ

79–06–156–6

FIG. 45
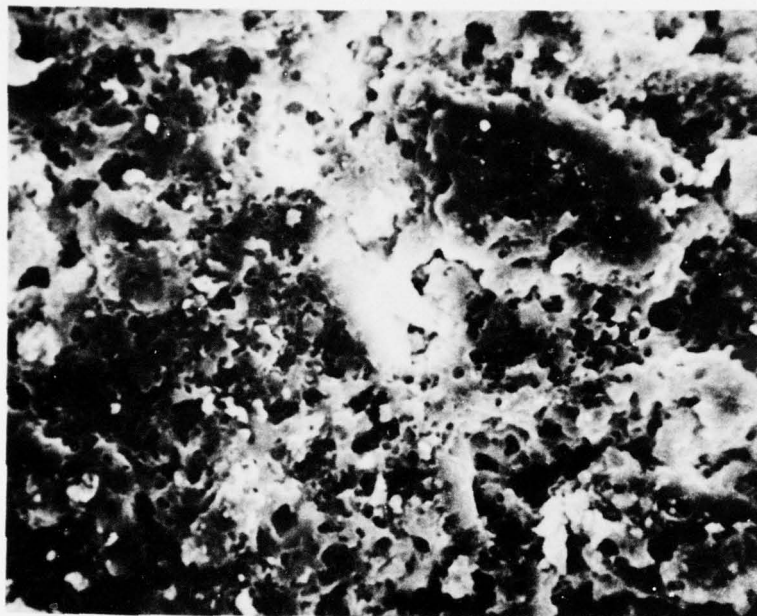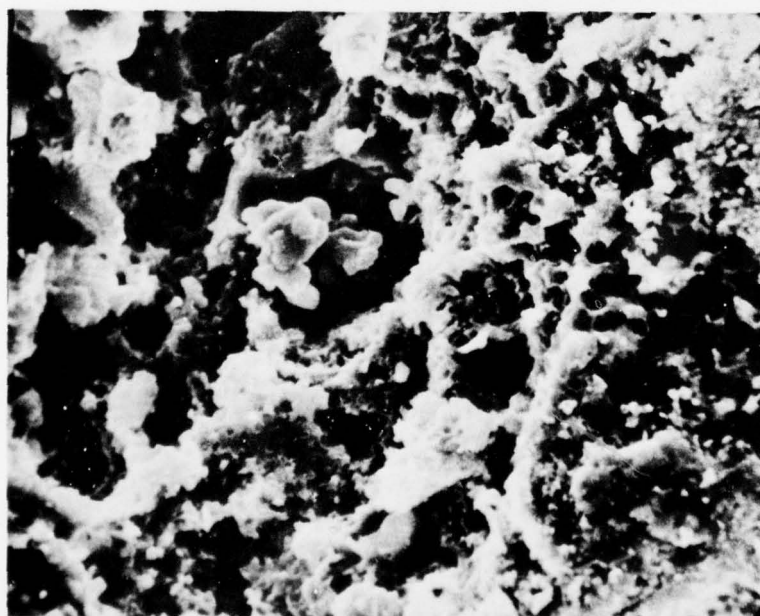
SURFACE OF CVD Si_3N_4 OVERLAYER ON A −200 RSSN/HPSN EROSION SAMPLE.

10μ

79–06–156–15

FIG. 46

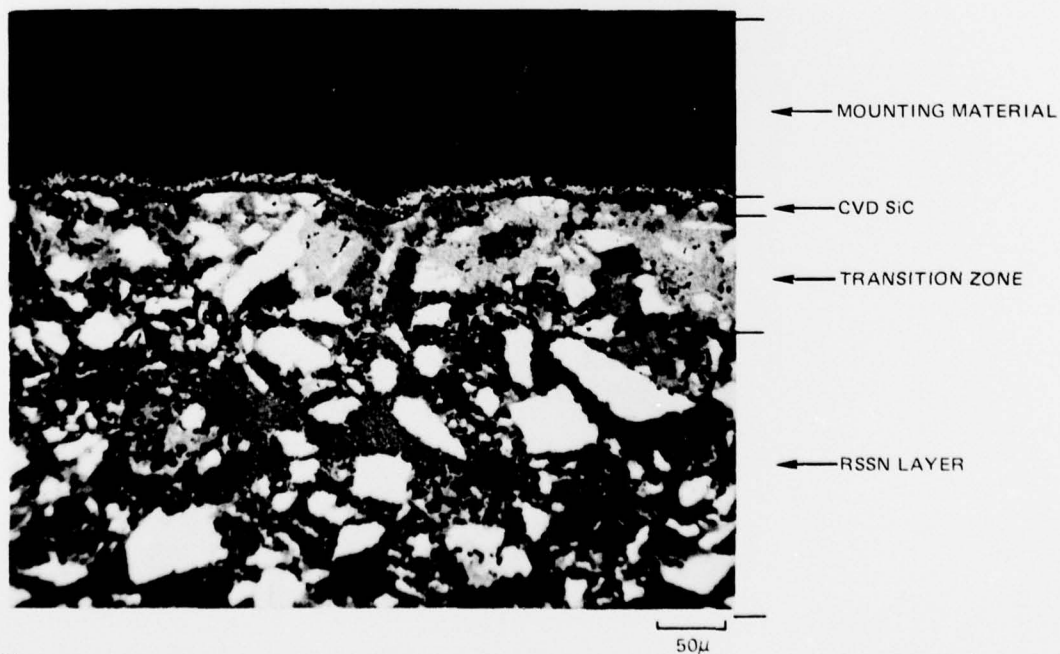CROSS—SECTION OF A CVD Si_3N_4 COATING DEPOSITED AT 1400ºC
ON −200 RSSN LAYER

50μ
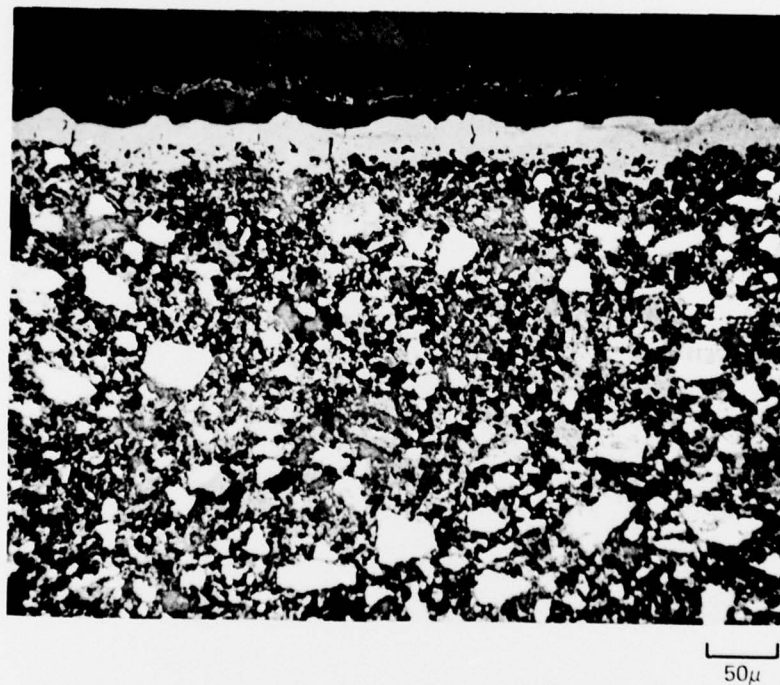
105

CROSS–SECTION OF A–200 RSSN LAYER WITH A CVD SiC OVERLAYER BEFORE (A)
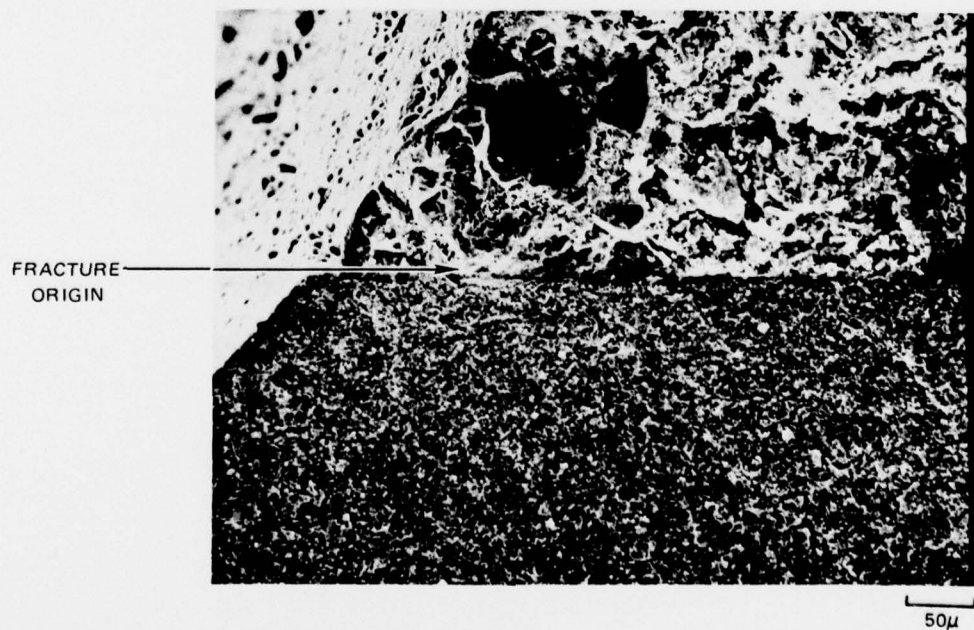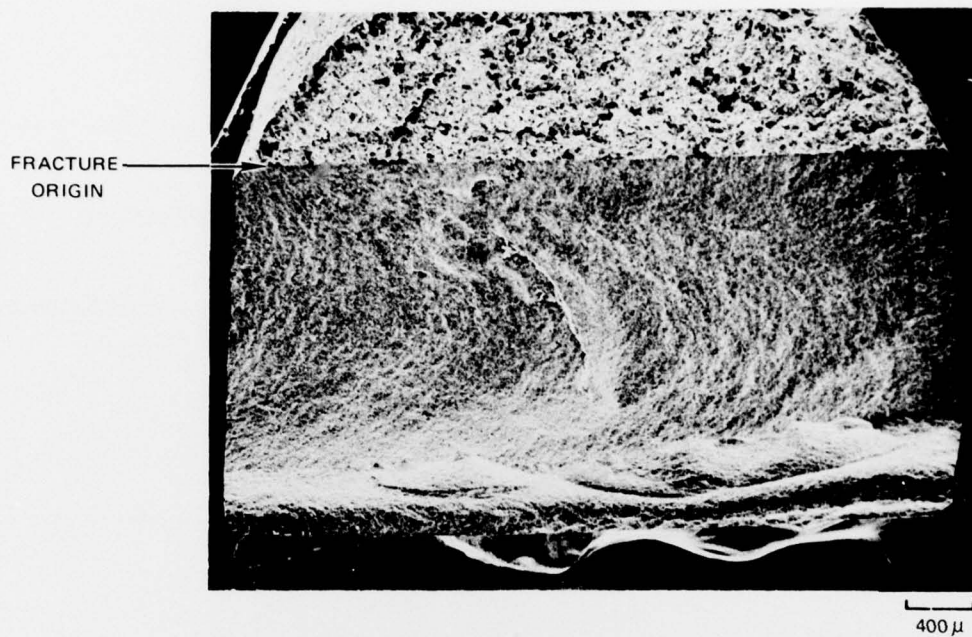AND AFTER (B) A 5 HR, 1370°C EROSION TEST

← MOUNTING MATERIAL

← CVD SiC

← TRANSITION ZONE

← RSSN LAYER

50μ

a)

← MOUNTING MATERIAL

← CVD SiC

← TRANSITION ZONE

← RSSN LAYER

50μ

b)

106

FIG. 48
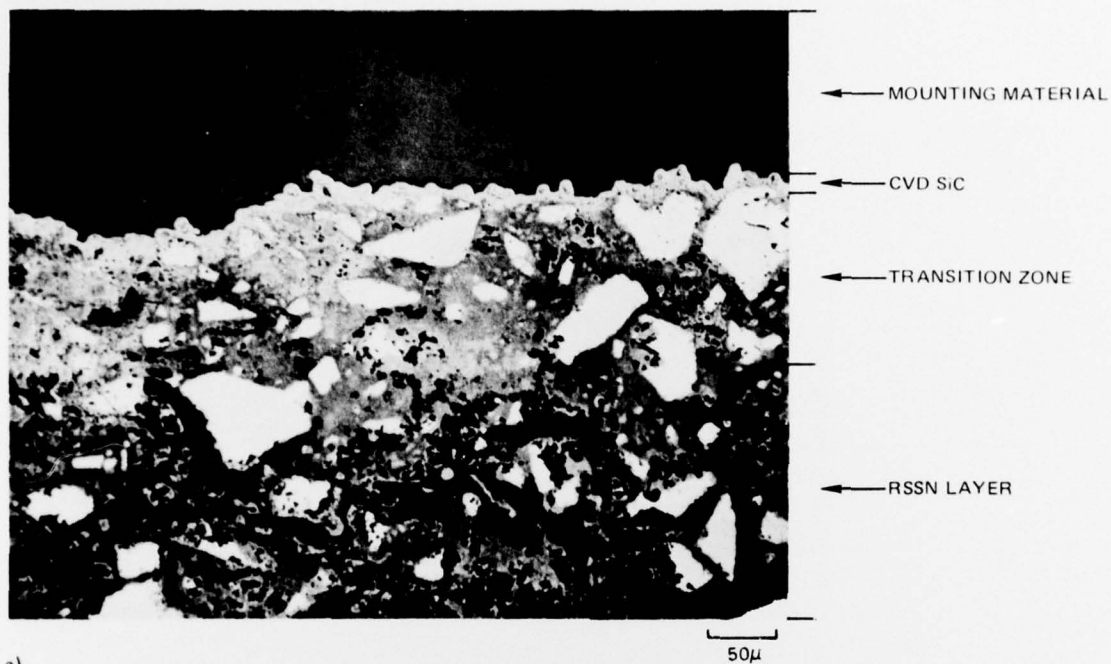
FRACTURE SURFACE OF −200 RSSN/HPSN COMBINATION
WITH CVD SiC OVERLAYER

FRACTURE ORIGIN

400 μ

FRACTURE ORIGIN

50μ

107

79-06-156-16

DATE
FILME